Eidgenössische Technische Hochschule Zürich

Ecole polytechnique fédérale de Zurich
Politecnico federale di Zurigo
Swiss Federal Institute of Technology Zurich

Convergence analysis of Finite Element Methods for $\mathbf{H}(\mathbf{curl}; \Omega)$-elliptic interface problems

R. Hiptmair, J. Li* and J. Zou†

Research Report No. 2009-04
January 2009

Seminar für Angewandte Mathematik
Eidgenössische Technische Hochschule
CH-8092 Zürich
Switzerland

*Department of Mathematics, The Chinese University of Hong Kong, Shatin, N.T., Hong Kong; jzli@math.cuhk.edu.hk.

†Department of Mathematics, The Chinese University of Hong Kong, Shatin, N.T., Hong Kong, zou@math.cuhk.edu.hk. The work of this author was substantially supported by Hong Kong RGC grants (Project 404407 and 404606).

Convergence Analysis of Finite Element Methods for $\boldsymbol{H}(\mathbf{curl};\Omega)$-elliptic Interface Problems

Ralf Hiptmair* Jingzhi Li† Jun Zou‡

January 21, 2009

Abstract

In this article we analyse a finite element method for solving $\boldsymbol{H}(\mathbf{curl};\Omega)$-elliptic interface problems in general three-dimensional polyhedral domains with smooth material interfaces. The continuous problems are discretized by means of the first family of lowest order Nédélec $\boldsymbol{H}(\mathbf{curl};\Omega)$-conforming finite elements on a family of tetrahedral meshes which resolve the smooth interface in the sense of sufficient approximation in terms of a parameter δ that quantifies the mismatch between the smooth interface and the triangulation. Optimal error estimates in the $\boldsymbol{H}(\mathbf{curl};\Omega)$-norm are obtained for the first time. The analysis is based on a so-called δ-strip argument, a new extension theorem for $\boldsymbol{H}^1(\mathbf{curl})$-functions across smooth interfaces, a novel non-standard interface-aware interpolation operator, and a perturbation argument for degrees of freedom for $\boldsymbol{H}(\mathbf{curl};\Omega)$-conforming finite elements. Numerical tests are presented to verify the theoretical predictions and confirm the optimal order convergence of the numerical solution.

Key words. $\boldsymbol{H}(\mathbf{curl};\Omega)$-elliptic interface problems, finite element methods, Nédélec's edge elements, convergence analysis.

AMS subject classification 2000. 65N12, 65N30, 35Q60

1 Introduction

Given a bounded polyhedral domain $\Omega \subset \mathbb{R}^3$ with a Lipschitz boundary, we assume that the domain Ω consists of two subdomains Ω_1 and Ω_2, where $\Omega_1 \subset\subset \Omega$, $\Omega_2 := \Omega \setminus \overline{\Omega}_1$. The internal interface $\Gamma := \partial\Omega_1$ is to be sufficiently smooth, namely, at least C^2-smooth (see Figure 1 for an illustration of the geometric setting). We are concerned with solving the $\boldsymbol{H}(\mathbf{curl};\Omega)$-elliptic interface problem

$$\mathbf{curl}\,\chi\,\mathbf{curl}\,\mathbf{u} + \beta\mathbf{u} = \mathbf{f} \quad \text{in } \Omega, \tag{1.1}$$

with Dirichlet boundary condition

$$\mathbf{n}\times\mathbf{u} = 0 \quad \text{on } \partial\Omega, \tag{1.2}$$

and jump conditions on the interface

$$[\mathbf{n}\times\mathbf{u}] = 0 \quad \text{on } \Gamma, \tag{1.3}$$

$$[\chi\mathbf{n}\times\mathbf{curl}\,\mathbf{u}] = 0 \quad \text{on } \Gamma\,, \tag{1.4}$$

*SAM, ETH, Zürich, CH-8092 Zürich, Switzerland (hiptmair@sam.math.ethz.ch).

†Department of Mathematics, The Chinese University of Hong Kong, Shatin, N.T., Hong Kong (jzli@math.cuhk.edu.hk).

‡Department of Mathematics, The Chinese University of Hong Kong, Shatin, N.T., Hong Kong. The work of this author was substantially supported by Hong Kong RGC grants (Project 404407 and 404606). (zou@math.cuhk.edu.hk).

where $\mathbf{f} \in \boldsymbol{L}^2(\Omega)$, β is a strictly positive constant, and χ is a scalar function of the spatial variable $\mathbf{x} \in \Omega$ and there are two constants $\underline{\chi}, \overline{\chi}$ with $0 < \underline{\chi} \leq \overline{\chi}$ such that $\underline{\chi} \leq \chi \leq \overline{\chi}$ a.e. in Ω. Further, $\mathbf{n}$ stands for a unit normal vector to the boundary $\partial\Omega_1$ pointing into Ω_2; and we denote by $[\mathbf{v}] := \mathbf{v}_1 - \mathbf{v}_2$ the jump of a vector-valued quantity $\mathbf{v}$ across the interface Γ (or by $[v] := v_1 - v_2$ the jump of a scalar v). For ease of exposition, we assume that the coefficient function χ is piecewise constant, i.e.

$$\chi(\mathbf{x}) = \begin{cases} \chi_1, & \mathbf{x} \in \Omega_1; \\ \chi_2, & \mathbf{x} \in \Omega_2, \end{cases}$$

where χ_i $(i = 1, 2)$ are positive constants. The more general case of piecewise smooth coefficient can be treated similarly with no essential difficulty by using techniques like averaging in an element.

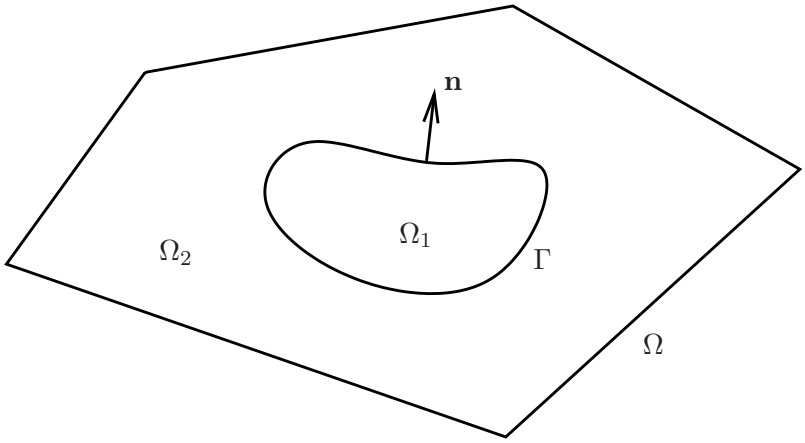

Figure 1: An illustrative sketch of the setting of the problem.

$\boldsymbol{H}(\mathbf{curl}; \Omega)$-elliptic interface problems like (1.1)–(1.4) have to be solved at each time step for the eddy current model, which typically arises from Maxwell's equations as a magneto-quasistatic approximation by dropping the displacement current (see, e.g., [2, 5, 14]), and is frequently used in low frequency, high-conductivity applications like electric machines. In this setting χ represents the magnetic susceptibility, whereas β is related to the conductivity. The homogeneous Dirichlet boundary condition (1.2) model perfectly conducting walls.

Due to the practical relevance of interface problems in many engineering and industrial applications, numerical solution methods for interface problems have been investigated widely. One may refer to a recent monograph [23] and the references therein for a history of the development on the topic. Numerous variants of finite element methods (FEMs) for classical elliptic interface problems in $H^1(\Omega)$ have been extensively studied in the past few decades. Interested readers may refer to [3, 7, 9, 11, 17, 21, 22, 28].

Nevertheless, to the best knowledge of the authors, there seems to exist no corresponding work on the convergence analysis of $\boldsymbol{H}(\mathbf{curl}; \Omega)$-elliptic interface problems discretized by means of interface-aligned edge elements. These $\boldsymbol{H}(\mathbf{curl}; \Omega)$-conforming finite elements are the natural choice for (1.1)–(1.4) and well capture the structure of $\boldsymbol{H}(\mathbf{curl}; \Omega)$-elliptic boundary value problem, see [18]. Yet, most existing analytic tools for $H^1(\Omega)$-elliptic interface problems based on Lagrangian nodal elements do not fit edge elements. Hence it is a non-trivial task to adapt some of these techniques and tools for the convergence analysis to the $\boldsymbol{H}(\mathbf{curl}; \Omega)$-setting.

The main contribution of the current work is to derive optimal order convergence in the $\boldsymbol{H}(\mathbf{curl}; \Omega)$-norm for $\boldsymbol{H}(\mathbf{curl}; \Omega)$-elliptic interface problems using lowest order Nédélec $\boldsymbol{H}(\mathbf{curl}; \Omega)$-conforming finite elements. To that end, some novel analytical tools and techniques have been developed, including a non-standard interface-aware finite element interpolant which will be shown to be a quasi-optimal projection in the sense of the $\boldsymbol{H}(\mathbf{curl}; \Omega)$ norm, a δ-strip argument for quantifying the relation of error estimate near the interface in terms of the mismatch parameter δ, a new extension theorem for $\boldsymbol{H}^1(\mathbf{curl}; \Omega_i)$ functions across smooth interfaces for $i = 1, 2$, which bridges the gap between standard and non-standard interpolation and thus is crucial for the argument of convergence, and a perturbation argument for the degrees of freedom for $\boldsymbol{H}(\mathbf{curl}; \Omega)$-conforming finite elements.

The remainder of the paper is organized as follows: In Section 2, we first introduce some necessary notations and assumptions to be used later, then derive the variational formulation for the $\boldsymbol{H}(\mathbf{curl};\Omega)$-elliptic interface problem, and present the finite element approximation using the lowest order Nédélec's $\boldsymbol{H}(\mathbf{curl};\Omega)$-conforming finite element spaces. In Section 3 we prepare some important theoretical results, including a δ-strip argument for error estimation near the interface and the construction of a new extension operator for $\boldsymbol{H}^1(\mathbf{curl};\Omega_i)$ functions across smooth interfaces for $i = 1, 2$. In Section 4, we prove the optimal order convergence in the sense of $\boldsymbol{H}(\mathbf{curl};\Omega)$-norm for $\boldsymbol{H}(\mathbf{curl};\Omega)$-elliptic interface problems. In Section 5, numerical experiments are presented to justify the predictions of the convergence theory. Conclusions and future work are addressed in Section 6.

2 Finite element approximation

In the sequel, we adopt the convention that roman letters denote scalar functions, and their associated spaces etc., while bold letters represent vector-valued functions, and their associated spaces etc. For the convenience of presentation, we first introduce the following function spaces that will be used throughout the paper:

$$\begin{aligned}
\boldsymbol{H}(\mathbf{curl};\Omega) &= \left\{ \mathbf{v} \in \boldsymbol{L}^2(\Omega) \mid \mathbf{curl}\,\mathbf{v} \in \boldsymbol{L}^2(\Omega) \right\}, \\
\boldsymbol{H}^1(\mathbf{curl};\Omega) &= \left\{ \mathbf{v} \in \boldsymbol{H}^1(\Omega) \mid \mathbf{curl}\,\mathbf{v} \in \boldsymbol{H}^1(\Omega) \right\}, \\
\boldsymbol{H}_0(\mathbf{curl};\Omega) &= \left\{ \mathbf{v} \in \boldsymbol{H}(\mathbf{curl};\Omega) \mid \mathbf{n} \times \mathbf{v} = 0 \text{ on } \partial\Omega \right\}.
\end{aligned}$$

The Hilbert spaces $\boldsymbol{H}(\mathbf{curl};\Omega)$ and $\boldsymbol{H}^1(\mathbf{curl};\Omega)$ are equipped with the canonical inner products and the associated norms. For the properties of these function spaces used in this paper we refer to [16, Chap. 1] or [25]. Similar notations will be used for Ω_1 and Ω_2, respectively.

For a scalar function $u \in L^2(\Omega)$ we denote by u_i its restriction to Ω_i, i.e., $u_i := u|_{\Omega_i}$, for $i = 1, 2$. While for a vector-valued function $\mathbf{u} = (u^1, u^2, u^3)^T \in \boldsymbol{L}^2(\Omega)$ we denote by $\mathbf{u}_i = (u_i^1, u_i^2, u_i^3)^T$ its restriction to Ω_i, i.e., $\mathbf{u}_i := \mathbf{u}|_{\Omega_i}$, for $i = 1, 2$, where $(\cdot)^T$ denotes the transpose operator.

2.1 Weak formulation

The weak formulation of (1.1)–(1.4) is straightforward and reads as follows:
Problem (P) Seek $\mathbf{u} \in \boldsymbol{H}_0(\mathbf{curl};\Omega)$ such that

$$a(\mathbf{u}, \mathbf{v}) = \int_\Omega \mathbf{f} \cdot \mathbf{v}\, \mathrm{d}\mathbf{x} \qquad \forall\, \mathbf{v} \in \boldsymbol{H}_0(\mathbf{curl};\Omega)\,, \tag{2.1}$$

with the bilinear form defined by

$$a(\mathbf{u}, \mathbf{v}) := \sum_{i=1}^{2} \int_{\Omega_i} \left(\chi_i\, \mathbf{curl}\,\mathbf{u}_i \cdot \mathbf{curl}\,\mathbf{v}_i + \beta \mathbf{u}_i \cdot \mathbf{v}_i\right) \mathrm{d}\mathbf{x}\,. \tag{2.2}$$

By the assumptions on χ and β in Sectioin 1, the bilinear forms $a(\cdot,\cdot)$ in (2.2) agrees with the $\boldsymbol{H}(\mathbf{curl};\Omega)$-inner product of the Hilbert space $\boldsymbol{H}_0(\mathbf{curl};\Omega)$ up to the weights χ_i and β, and the associated energy norm $\|\mathbf{u}\|_a = a(\mathbf{u}, \mathbf{u})^{1/2}$ is equivalent to the $\boldsymbol{H}(\mathbf{curl};\Omega)$-norm in the following sense

$$c\, \|\mathbf{u}\|_{\boldsymbol{H}(\mathbf{curl};\Omega)} \le \|\mathbf{u}\|_a \le C\, \|\mathbf{u}\|_{\boldsymbol{H}(\mathbf{curl};\Omega)}\,, \tag{2.3}$$

where $c = \min(\chi_1, \chi_2, \beta)$ and $C = \max(\chi_1, \chi_2, \beta)$. This ensures the existence and uniqueness of the solution of (2.1) by the Lax-Milgram Lemma [12, Theorem 1.1.3].

As suggested by [13], we make the reasonable assumption that the solution of (2.1) belongs to $\boldsymbol{H}_0(\mathbf{curl};\Omega) \cap \boldsymbol{H}^1(\mathbf{curl};\Omega_1) \cap \boldsymbol{H}^1(\mathbf{curl};\Omega_2)$. Theoretical results for more general setting, namely $\boldsymbol{H}_0(\mathbf{curl};\Omega) \cap \boldsymbol{H}^s(\mathbf{curl};\Omega_1) \cap \boldsymbol{H}^s(\mathbf{curl};\Omega_2)$ for $0 \le s \le 1$, will also be investigated at the end of Section 4. They require suitable fractional Sobolev spaces defined by the method of real interpolation. Interested readers may refer to a separate work [19] for more details.

2.2 Triangulation

Let the polyhedral domain $\Omega \in \mathbb{R}^3$ be equipped with a family of oriented unstructured tetrahedral meshes $(\mathcal{T}_h)_h$ in the sense of [18, Def. 3], where h stands for the meshsize. There are no nestedness requirement for the family of triangulations, which concerns a practical issue to be addressed in Section 5. We denote by $\mathcal{F}_h$, $\mathcal{E}_h$ and $\mathcal{N}_h$ the respective sets of faces, edges and nodes related to the triangulation $\mathcal{T}_h$. The quality of $\mathcal{T}_h$ can be gauged by means of its meshsize h, shape regularity measure $\rho(\mathcal{T}_h)$and quasi-uniformity measure $\gamma(\mathcal{T}_h)$ [10, Sect. 3] as follows

$$\rho(\mathcal{T}_h) := \max_{K\in\mathcal{T}_h} \frac{h_K}{r_K}, \quad h := \max_{K\in\mathcal{T}_h} h_K, \quad \gamma(\mathcal{T}_h) := \max_{K\in\mathcal{T}_h} \frac{h}{h_K},$$

where

$$\begin{aligned} h_K &:= \max\{|\mathbf{x}-\mathbf{y}| : \mathbf{x},\mathbf{y}\in K\}\,, \\ r_K &:= \max\{r>0 : \exists \mathbf{x}\in K;\, |\mathbf{x}-\mathbf{y}|<r \Rightarrow \mathbf{y}\in K\}\,. \end{aligned}$$

Afterward, we will frequently denote by c and C generic positive constants which may depend on the domain Ω, the coefficients χ_i's, β and the shape-regularity measure $\rho(\mathcal{T}_h)$, but must not depend on the mesh size h and the related functions.

In the rest of this subsection, let us explain our assumptions on the meshes in turns. First of all, our finite element discretization scheme relies heavily on the concept of *interface-aligned triangulation*, which can be understood as follows.

Assumption 2.1. *The triangulation $\mathcal{T}_h$ is* interface-aligned *if for every $K \in \mathcal{T}_h$* all *its four vertices are either in $\overline{\Omega}_1$ or in $\overline{\Omega}_2$, and this element K is assumed to intersect with the interface Γ in such a way that at most three of its vertices are located on the interface Γ while all remaining vertices are either in Ω_1 or in Ω_2.*

From now on, a vertex in $\mathcal{N}_h$ located on the interface is called an *interface vertex*, an edge in $\mathcal{E}_h$ with two end nodes on the interface an *interface edge*. Let us comment on Assumption 2.1 before we proceed. To meet the requirement of Assumption 2.1, the triangulation $\mathcal{T}_h$ should not be too coarse with respect to the interface, i.e., it is not allowed to let all the four vertices of an element $K \in \mathcal{T}_h$ located on the interface Γ. This might be the case for a region with large curvature on the interface. Nevertheless, we can always refine the mesh until all the elements in the mesh satisfies Assumption 2.1 owing to the smoothness of the interface.

When an element K satisfies $\overline{K} \cap \Gamma \neq \emptyset$, it is called an interface element, otherwise a non-interface element. The set of all interface elements is denoted by $\mathcal{T}_* := \{\, K \in \mathcal{T}_h \,|\, \overline{K} \cap \Gamma \neq \emptyset \,\}$ and $\mathcal{T}_*^i := \{\, K \in \mathcal{T}_* \,|\, \text{all nodes of } K \text{ are in } \overline{\Omega}_i \,\}$ represents the set of all interface elements of Ω_i, for $i = 1, 2$. For some small $\delta > 0$, we define the *δ-strip regions* around the interface in Ω and Ω_i, $i = 1, 2$, respectively, by

$$S_\delta := \{\, x \in \Omega \,|\, \mathrm{dist}(x,\Gamma) < \delta \,\}, \quad S_\delta^i := \{\, x \in \Omega_i \,|\, \mathrm{dist}(x,\Gamma) < \delta \,\}, \quad i = 1, 2.$$

It is obvious that $S_\delta = S_\delta^1 \cup S_\delta^2$ and these δ-strip regions will be used to bound the error near the interface, which cannot be captured by standard interpolation error estimates.

Of course, the smooth interface Γ can only be approximately resolved by tetrahedral meshes. We quantify the quality of the approximation of the smooth interface Γ by the triangulation $\mathcal{T}_h$ in terms of a parameter δ through the following definition.

Definition 2.2. *The triangulation $\mathcal{T}_h$ is said to resolve the interface Γ* up to the error *δ if it can be decomposed as $\mathcal{T}_h = \mathcal{T}^1 \cup \mathcal{T}^2 \cup \mathcal{T}_*^1 \cup \mathcal{T}_*^2$, where*

$$\mathcal{T}^i = \{\, K \in \mathcal{T}_h \,;\quad K \subset \Omega_i \setminus S_\delta \,\}\,,$$

and $K \in \mathcal{T}_*^i$ if

$$\max\{\, \mathrm{dist}(x, \Gamma \cap K) \,;\quad x \in \overline{K} \cap \overline{\Omega}_{i'} \,\} \le \delta\,,$$

for $i = 1, 2$, and we define its dual i' as follows: $i' = 1$ if $i = 2$ and $i' = 2$ if $i = 1$.

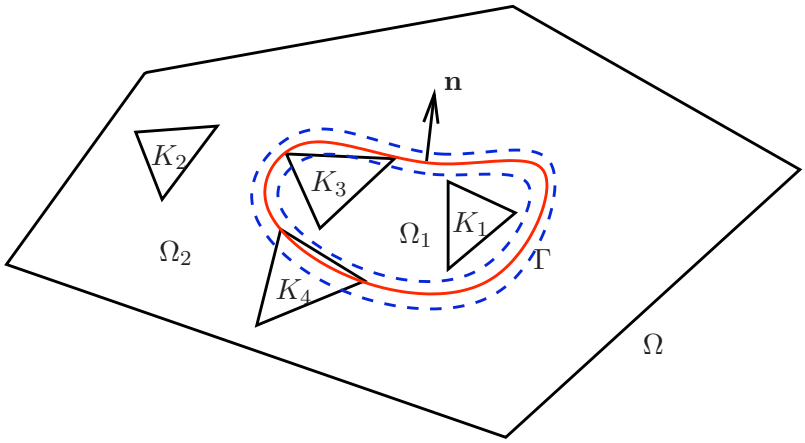

Figure 2: S_δ: the region of width 2δ between the two blue closed dashed lines around the interface Γ in red. Interface elements: $K_3 \in \mathcal{T}_*^1$, $K_4 \in \mathcal{T}_*^2$. Non-interface elements: $K_1 \in \mathcal{T}^1$, $K_2 \in \mathcal{T}^2$.

We may refer to Figure 2 for a 2D illustration of Definition 2.2. Note that although we assume that all vertices of an element K must belong to either subdomain Ω_1 or Ω_2. It is possible that the interface may cut some elements into two parts lying in two different subdomains, see, for instance, triangle K_4 in Figure 2. By Definition 2.2 we easily see that any interface element K can be embedded in the union of the interface strip S_δ and one of the subdomains Ω_1 and Ω_2.

For a smooth interface Γ approximated by a union of triangular faces of the triangulation $\mathcal{T}_h$, we may further quantify the parameter δ in terms of the meshsize h as given by the next assumption.

Assumption 2.3. *The interface Γ is at least C^2-smooth. For the interface-aligned meshes, there exists some δ of order h^2 such that $K \cap \Omega_2 \subset S_\delta^2$ for all elements $K \in \mathcal{T}_*^1$, and $K \cap \Omega_1 \subset S_\delta^1$ for all elements $K \in \mathcal{T}_*^2$.*

A detailed proof of Assumption 2.3 of δ-approximation property for the interface-aligned triangulation in two dimensions can be found in [11] and the same idea can be extended to 3D with no essential changes.

For the subsequent error estimate, we have to resort to an important auxiliary concept for the definition of the perturbed interpolation operator.

Definition 2.4 (Interface twin edge)**.** *For any interface edge $e \in \mathcal{E}_h$, there exist two interface elements K_1 and K_2, with non-interface vertices $\mathbf{p}_1$ and $\mathbf{p}_2$, respectively, which share the interface edge e and another interface node $\mathbf{q}$, such that there is a unique curve $\widetilde{e}$ which is the intersection by the interface and two triangular faces determined by $\mathbf{p}_1$ with e, and $\mathbf{p}_2$ with e, respectively. We call $\widetilde{e}$ the* interface twin edge *associated with the interface edge e (see Figure 3).*

Basically, the interface edge e is a straight segment, and the interface twin edge $\widetilde{e}$ is a piecewise smooth curve as represented by the alternating red and blue smooth curves which shares two end nodes and possibly some other points with the interface edge e. (see Figure 3).

Remark 2.5. *Observe that face areas bounded by the interface edge e and its twin one $\widetilde{e}$ are still contained within the δ-region. Specifically, let us denote by $S_{e,\widetilde{e}}$ the piecewise planar surface bounded by the curves e and $\widetilde{e}$ as shown in Figure 3. It is readily seen by Assumption 2.3 that*

$$S_{e,\widetilde{e}} \subset S_\delta. \tag{2.4}$$

In the subsequent lemmas, theorems, and proofs, etc., two additional technical assumptions are made. First, the triangulation $\mathcal{T}_h$ is assumed to be quasi-uniform in the sense of [12], namely, $\gamma(\mathcal{T}_h)$ is bounded from above by some constant. It is obvious that the bound for $\gamma(\mathcal{T}_h)$ implies a bound of $\rho(\mathcal{T}_h)$, which imposes a limitation on the number of tetrahedra sharing a vertex, an edge, and a face [12]. Second, the triangulation $\mathcal{T}_h$ is assumed to be sufficiently fine to allow the existence of interface twin edges. For some interface with bizarre geometry the interface twin edges might not be

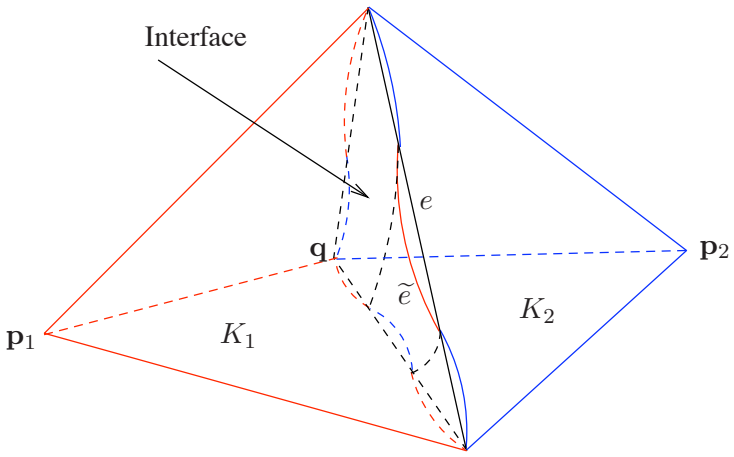

Figure 3: Two typical interface elements K_1 and K_2 intersect with the interface Γ. Interface edges are plotted by black straight lines on the interface. Interface twin edges are visualized as the piecewise smooth curves composed of blue and read curved segments.

well defined for certain coarse meshes. Nevertheless, the smoothness of the interface makes it look *flat* from a local point of view. Thus we can always refine the mesh until a well-defined interface twin edge is obtained.

2.3 Finite element discretization

A suitable trial space $\mathbf{E}_h \subset \boldsymbol{H}_0(\mathbf{curl};\Omega)$ for the Galerkin discretization of (2.1) is supplied by the lowest order $\boldsymbol{H}(\mathbf{curl};\Omega)$-conforming edge elements of the first family due to Nédélec [18, 26], that is,

$$\mathbf{E}_h := \left\{ \mathbf{v}_h \in \boldsymbol{H}_0(\mathbf{curl};\Omega) \mid \mathbf{v}_h|_K(\mathbf{x}) = \mathbf{a}_K + \mathbf{b}_K \times \mathbf{x},\, \mathbf{a}_K, \mathbf{b}_K \in \mathbb{R}^3, \mathbf{x} \in K\ \forall K \in \mathcal{T}_h \right\} .$$

Writing $\widehat{\mathcal{E}}_h$ for the set of all interior edges of $\mathcal{T}_h$, the degrees of freedom of $\mathbf{E}_h$ are given by the path integrals

$$\mathbf{v}_h \mapsto \int_e \mathbf{v}_h \cdot \mathrm{d}\vec{s}\,, \quad e \in \widehat{\mathcal{E}}_h\,.$$

It is well established that there exists a well-defined global finite element interpolation operator $\mathbf{I}_h : \boldsymbol{H}^1(\mathbf{curl};\Omega) \mapsto \mathbf{E}_h$ [25, Thm. 5.41, Sect. 5.4] which has the following approximation property.

Lemma 2.6. *Let $(\mathcal{T}_h)_h$ be a family of quasi-uniform, oriented unstructured tetrahedral meshes on Ω. Then the interpolant $\mathbf{I}_h\mathbf{u}$ possesses the optimal approximation property:*

$$\|\mathbf{u} - \mathbf{I}_h\mathbf{u}\|_{\boldsymbol{H}(\mathbf{curl};\Omega)} \leq Ch\|\mathbf{u}\|_{\boldsymbol{H}^1(\mathbf{curl};\Omega)} \quad \forall\, \mathbf{u} \in \boldsymbol{H}^1(\mathbf{curl};\Omega)\,. \tag{2.5}$$

Moreover, we recall that edge elements are an affine equivalent family of finite elements with respect to the pullback transformation, see [18, 25],

$$\widehat{\mathbf{v}}(\widehat{\mathbf{x}}) := \mathsf{B}^T\mathbf{v}(\mathbf{x})\,, \quad \mathbf{x} = \mathsf{B}\widehat{\mathbf{x}} + \mathbf{t}\,, \quad \mathsf{B} \in \mathbb{R}^{3,3},\, \mathbf{t} \in \mathbb{R}^3\,.$$

On a tetrahedron K with barycentric coordinates $\lambda_1, \ldots, \lambda_4$, the local shape functions of $\mathbf{E}_h$ are given by (see [18, Sect. 3.2])

$$\lambda_i\, \mathbf{grad}\, \lambda_j - \lambda_j\, \mathbf{grad}\, \lambda_i\,, \quad 1 \leq i < j \leq 4\,.$$

They can be assembled into a basis $\{\mathbf{b}_e,\ e \in \widehat{\mathcal{E}}_h\}$ of $\mathbf{E}_h$.

With the finite element function spaces presented above, the finite element approximation of (2.1) can be stated as follows:

Problem ($\mathbf{P}_h$) Seek $\mathbf{u}_h \in \mathbf{E}_h$ such that

$$a(\mathbf{u}_h, \mathbf{v}_h) = \int_\Omega \mathbf{f} \cdot \mathbf{v}_h \, \mathrm{d}\mathbf{x} \qquad \forall\, \mathbf{v}_h \in \mathbf{E}_h \ . \tag{2.6}$$

The existence and uniqueness of the solution of (2.6) follows from the Lax-Milgram Lemma [12, Theorem 1.1.3], similar to those of the continuous problem ($\mathbf{P}$).

The practical evaluation of the stiffness matrix associated with the bilinear form $a(\cdot,\cdot)$ in (2.6) can be very complicated on an interface element when it is cut through by the interface, especially in three dimensions. A much more convenient formulation is obtained by replacing the original bilinear form (2.2) with an approximate bilinear form $a_h(\cdot,\cdot)$:

$$a_h(\mathbf{u}, \mathbf{v}) = \sum_{K \in \mathcal{T}} \int_K \left(\chi_K \, \mathbf{curl}\, \mathbf{u} \cdot \mathbf{curl}\, \mathbf{v} + \beta \mathbf{u} \cdot \mathbf{v}\right) \mathrm{d}\mathbf{x}\,, \tag{2.7}$$

where the coefficients χ_K are elementwise constant. In our present setting of piecewise constant coefficient χ, for every $K \in \mathcal{T}$, χ_K is taken to be χ_i if $K \in \mathcal{T}^i$ or $\mathcal{T}^i_*$ when $i \in \{1, 2\}$.

With the modified bilinear form in (2.7), we can now define a more practical finite element method for the variational problem (P).

Problem ($\widetilde{\mathbf{P}}_h$) Find $\mathbf{u}_h \in \mathbf{E}_h$ such that

$$a_h(\mathbf{u}_h, \mathbf{v}_h) = \int_\Omega \mathbf{f} \cdot \mathbf{v}_h \, \mathrm{d}\mathbf{x} \qquad \forall\, \mathbf{v}_h \in \mathbf{E}_h. \tag{2.8}$$

It can be immediately seen that the bilinear form $a_h(\cdot,\cdot)$ still preserves coercivity and continuity, and thus the well-posedness of Problem ($\widetilde{\mathbf{P}}_h$) is assured. Moreover, the two bilinear forms a_h and a are related to each other by

$$a(\mathbf{u}, \mathbf{v}) = a_h(\mathbf{u}, \mathbf{v}) + a^\Delta(\mathbf{u}, \mathbf{v}), \tag{2.9}$$

where the bilinear form $a^\Delta(\cdot,\cdot)$ satisfies

$$|a^\Delta(\mathbf{u}, \mathbf{v})| \le C \|\mathbf{u}\|_{\boldsymbol{H}(\mathbf{curl}; S_\delta)} \|\mathbf{v}\|_{\boldsymbol{H}(\mathbf{curl}; S_\delta)} \tag{2.10}$$

with the constant C depending only on the coefficients χ_i's and β.

2.4 Interface-aware interpolation operator

It is worth remarking that there are no ambiguities of the interpolation operator $\mathbf{I}_h$ when applied for functions in $\boldsymbol{H}_0(\mathbf{curl}; \Omega) \cap \boldsymbol{H}^1(\mathbf{curl}; \Omega_1) \cap \boldsymbol{H}^1(\mathbf{curl}; \Omega_2)$, but the corresponding interpolant is not a good candidate for investigating best approximation estimates. Instead we shall define a problem-specific interface-aware interpolation operator, which can be viewed as a perturbed version of $\mathbf{I}_h$. The crux here is to define a perturbed degree of freedom for each interface edge of an interface element through a surrogate degree of freedom defined along the interface twin edge. To be more precise, we elucidate the idea in the following definition.

Definition 2.7 (Interface-aware interpolation operators)**.** *Let $\mathcal{T}_h$ be an oriented unstructured tetrahedral triangulation satisfying Assumptions 2.1 and 2.3 with mesh size h, and $\mathbf{E}_h$ the lowest order Nédélec $\boldsymbol{H}(\mathbf{curl}; \Omega)$-conforming edge element spaces of the first family on $\mathcal{T}_h$.*

For a function $\mathbf{u} \in \boldsymbol{H}_0(\mathbf{curl}; \Omega) \cap \boldsymbol{H}^1(\mathbf{curl}; \Omega_1) \cap \boldsymbol{H}^1(\mathbf{curl}; \Omega_2)$, we define a perturbed $\mathbf{E}_h$ *Interface-aware interpolation operator*

$$\widetilde{\mathbf{I}}_h : \boldsymbol{H}_0(\mathbf{curl}; \Omega) \cap \boldsymbol{H}^1(\mathbf{curl}; \Omega_1) \cap \boldsymbol{H}^1(\mathbf{curl}; \Omega_2) \mapsto \mathbf{E}_h$$

and its interpolant $\widetilde{\mathbf{I}}_h \mathbf{u}$ as follows:

1. *For any* non-interface *edge $e \in \widehat{\mathcal{E}}_h$, we set the degree of freedom associated with the basis function $\mathbf{b}_e$ along the edge e to be $\int_e \widetilde{\mathbf{I}}_h \mathbf{u} \cdot \mathrm{d}\vec{s} := \int_e \mathbf{u} \cdot \mathrm{d}\vec{s}$.*
2. *For any* interface *edge $e \in \widehat{\mathcal{E}}_h$ with the corresponding interface twin edge $\widetilde{e}$, we set the degree of freedom associated with the basis function $\mathbf{b}_e$ along the edge e to be $\int_e \widetilde{\mathbf{I}}_h \mathbf{u} \cdot \mathrm{d}\vec{s} := \int_{\widetilde{e}} \mathbf{u} \cdot \mathrm{d}\vec{s}$.*

We remark that the interface-aware interpolation operator $\widetilde{I}_h$ is introduced only for the subsequent error estimates, and it is not needed in the numerical implementation of the finite element method ($\widetilde{\mathbf{P}}_h$).

3 Theoretical tools

In this section, we supply some technical results which are indispensable tools for the convergence analysis of finite element methods for $\boldsymbol{H}(\mathbf{curl};\Omega)$-elliptic interface problems.

3.1 δ-strip argument

We first present a δ-strip argument which is used for the error estimate in the region near the interface and first appeared in [22, Lemma 3.4].

Lemma 3.1. *Let $i \in \{1,2\}$. Then it holds for any $z_i \in H^1(\Omega_i)$ that*

$$\|z_i\|_{L^2(S_\delta^i)} \leq C\sqrt{\delta}\|z_i\|_{H^1(\Omega_i)},$$

provided that δ is sufficiently small. Here the constant C depends only on the curvature of the smooth interface and the domain Ω.

There is a straightforward corollary to Lemma 3.1 which can be viewed as its vectorized version in $\boldsymbol{H}^1(\mathbf{curl})$ spaces by simply using the Cauchy-Schwarz inequality.

Corollary 3.2. *Let $i \in \{1,2\}$. Then it holds for any $z_i \in \boldsymbol{H}^1(\mathbf{curl};\Omega_i)$ that*

$$\|z_i\|_{\boldsymbol{H}(\mathbf{curl};S_\delta^i)} \leq C\sqrt{\delta}\|z_i\|_{\boldsymbol{H}^1(\mathbf{curl};\Omega_i)}$$

provided that δ is sufficiently small. The constant C depends only on the curvature of the smooth interface and the domain Ω.

3.2 A new extension theorem

Motivated by the construction of extension operators for functions in Sobolev spaces $H^k(\Omega)$ [1, 15], in this subsection we propose a new extension for functions in the space $\boldsymbol{H}^1(\mathbf{curl})$. This new extension will play a crucial role in the subsequent error estimate on interface elements.

The following extension theorem can be found in [15, Theorem 1, Sec. 5.4].

Theorem 3.3 (H^2-extension theorem)**.** *Assuming that U is a simply connected bounded domain in $\mathbb{R}^3$ with C^2-smooth boundary ∂U. Choose a bounded open set V such that $U \subset\subset V$. Then there exists a bounded linear extension operator*

$$E : H^2(U) \to H^2(\mathbb{R}^3)$$

such that for any scalar function $u \in H^2(U)$:

1. *$Eu = u$ a.e. in U.*
2. *Eu has support within V.*
3. *$\|Eu\|_{H^2(\mathbb{R}^3)} \leq C\|u\|_{H^2(U)}$ with the constant C depending only on U and V.*

Compared with the extension of scalar functions, vector fields must be extended in a more delicate way to conserve their properties. Consider a vector field $\mathbf{u} \in \boldsymbol{H}^1(\mathbf{curl};U)$. We wish to extend $\mathbf{u}$ to a global $\widetilde{\mathbf{u}} \in \boldsymbol{H}^1(\mathbf{curl};\mathbb{R}^3)$. Since for a scalar function $p \in H^2(U)$ we have $\mathbf{grad}\, p \in \boldsymbol{H}^1(\mathbf{curl};U)$, it looks promising to define an $\boldsymbol{H}^1(\mathbf{curl})$-extension operator $\mathbf{E}_{\mathbf{curl}}$ based on the commuting diagram property [18]:

$$\mathbf{E}_{\mathbf{curl}}(\mathbf{grad}\, p) = \mathbf{grad}(Ep). \tag{3.1}$$

It is obvious that the operator $\mathbf{E}_{\mathbf{curl}}$ defined in the form (3.1) preserves the $\mathbf{curl}$-free property of a grad field in U. While for general vector fields, we can exploit the structure of (3.1) to construct a universal extension operator $\mathbf{E}_{\mathbf{curl}}$ taking the cue from (3.1).

With the motivation above, now we can establish the $\boldsymbol{H}^1(\mathbf{curl})$-extension theorem across the C^2-smooth boundary.

Theorem 3.4. *Assuming that U is a connected bounded domain in $\mathbb{R}^3$ with C^2-smooth boundary ∂U. Choose a bounded open set V such that $U \subset\subset V$. Then there exists a bounded linear extension operator:*

$$\mathbf{E}_{\mathbf{curl}} \,:\, \boldsymbol{H}^1(\mathbf{curl}; U) \to \boldsymbol{H}^1(\mathbf{curl}; \mathbb{R}^3), \tag{3.2}$$

such that for each $\mathbf{u} \in \boldsymbol{H}^1(\mathbf{curl}; U)$:

1. $\mathbf{E}_{\mathbf{curl}}\mathbf{u} = \mathbf{u}$ *a.e. in* U.
2. $\|\mathbf{E}_{\mathbf{curl}}\mathbf{u}\|_{\boldsymbol{H}^1(\mathbf{curl};\mathbb{R}^3)} \le C\,\|\mathbf{u}\|_{\boldsymbol{H}^1(\mathbf{curl};U)}$, *with the constant C depending only on U and V.*

Proof. We first construct a special extension from within a half ball. For a fixed $\mathbf{x}^0 \in \partial U$, we first suppose that ∂U is flat near $\mathbf{x}^0$ which is lying in the plane $\{\mathbf{x} \in \mathbb{R}^3 \mid x_3 = 0\}$. Let us assume that there exists an open ball $B = \{\mathbf{x} \in \mathbb{R}^3; |\mathbf{x} - \mathbf{x}^0| < r\}$ with center $\mathbf{x}_0$ and radius $r > 0$ such that

$$\begin{cases} B^+ := B \cap \{x_3 \ge 0\} \subset \overline{U}, \\ B^- := B \cap \{x_3 < 0\} \subset \Omega \setminus \overline{U}. \end{cases}$$

Suppose $p \in C^\infty(\overline{U})$. A second-order reflection of p from B^+ to B^- can be obtained as follows:

$$\widetilde{p}(\mathbf{x}) := \begin{cases} p(\mathbf{x}), & \text{if } \mathbf{x} \in B^+; \\ \sum_{j=1}^3 \lambda_j p(x_1, x_2, -\frac{x_3}{j}), & \text{if } \mathbf{x} \in B^-, \end{cases}$$

where $(\lambda_1, \lambda_2, \lambda_3) = (6, -32, 27)$ is the unique solution of the 3×3 system of linear equations

$$\sum_{j=1}^3 (-\frac{1}{j})^k \lambda_j = 1, \quad k = 0, 1, 2\,. \tag{3.3}$$

With this special choice of λ's, it is straightforward to check that $\widetilde{p} \in C^2(B)$.

Now we define a reflection of $\mathbf{grad}\, p$ from B^+ to B^- based on (3.1), that is,

$$\widetilde{\mathbf{grad}\, p} := \begin{cases} \mathbf{grad}\, p, & \text{if } \mathbf{x} \in B^+; \\ \mathbf{grad}\, \widetilde{p}, & \text{if } \mathbf{x} \in B^-, \end{cases} \tag{3.4}$$

or written in the vector form,

$$\widetilde{\mathbf{grad}\, p}(\mathbf{x}) = \begin{cases} \begin{pmatrix} p_{x_1} \\ p_{x_2} \\ p_{x_3} \end{pmatrix}, & \text{if } \mathbf{x} \in B^+; \\ \begin{pmatrix} \sum_{j=1}^3 \lambda_j p_{x_1}(x_1, x_2, -\frac{x_3}{j}) \\ \sum_{j=1}^3 \lambda_j p_{x_2}(x_1, x_2, -\frac{x_3}{j}) \\ \sum_{j=1}^3 -\frac{\lambda_j}{j} p_{x_3}(x_1, x_2, -\frac{x_3}{j}) \end{pmatrix}, & \text{if } \mathbf{x} \in B^-. \end{cases} \tag{3.5}$$

Comparing the components of $\widetilde{\mathbf{grad}\, p}$ in (3.5) in the B^+ and B^-, we can construct a tentative extension formula for a general vector field $\mathbf{w}(\mathbf{x}) = (w^1(\mathbf{x}), w^2(\mathbf{x}), w^3(\mathbf{x}))^T \in \boldsymbol{C}^\infty(B^+)$ in the following form,

$$\widetilde{\mathbf{w}}(\mathbf{x}) = \begin{pmatrix} \widetilde{w^1}(\mathbf{x}) \\ \widetilde{w^2}(\mathbf{x}) \\ \widetilde{w^3}(\mathbf{x}) \end{pmatrix} := \begin{cases} \mathbf{w}(\mathbf{x}), & \text{if } \mathbf{x} \in B^+; \\ \begin{pmatrix} \sum_{j=1}^3 \lambda_j w^1(x_1, x_2, -\frac{x_3}{j}) \\ \sum_{j=1}^3 \lambda_j w^2(x_1, x_2, -\frac{x_3}{j}) \\ \sum_{j=1}^3 -\frac{\lambda_j}{j} w^3(x_1, x_2, -\frac{x_3}{j}) \end{pmatrix}, & \text{if } \mathbf{x} \in B^-, \end{cases} \tag{3.6}$$

where $(\lambda_1, \lambda_2, \lambda_3)$ are as above. We claim $\widetilde{\mathbf{w}} \in \boldsymbol{C}^1(B)$ and, thus, $\mathbf{curl}\,\widetilde{\mathbf{w}} \in \boldsymbol{C}^0(B)$. A detailed computation confirms this by observing the relations (3.3), (3.6) and the following agreement of limits from both sides

$$\begin{aligned}\lim_{x_3\to 0+} \widetilde{w^i}(\mathbf{x}) &= \lim_{x_3\to 0-} \widetilde{w^i}(\mathbf{x}) \qquad i=1,2,3,\\ \lim_{x_3\to 0+} \widetilde{w^i}_{x_j}(\mathbf{x}) &= \lim_{x_3\to 0-} \widetilde{w^i}_{x_j}(\mathbf{x}) \quad i,j=1,2,3.\end{aligned}$$

With this tentative extension $\widetilde{\mathbf{w}}$ on hand, it is necessary to show the resulting extension from $\boldsymbol{H}^1(\mathbf{curl}; B^+)$ to $\boldsymbol{H}^1(\mathbf{curl}; B)$ is continuous. It is rather straightforward to show that $\|\widetilde{\mathbf{w}}\|_{\boldsymbol{H}^1(B)} \le C\,\|\mathbf{w}\|_{\boldsymbol{H}^1(B+)}$ by collecting coefficients and using the mirror reflection, that is,

$$\begin{aligned}&\int_B |\widetilde{\mathbf{w}}(\mathbf{x})|^2\,\mathrm{d}\mathbf{x} + \int_B |\,\mathbf{grad}\,\widetilde{\mathbf{w}}(\mathbf{x})|^2\,\mathrm{d}\mathbf{x}\\ &= \int_{B^+} |\mathbf{w}(\mathbf{x})|^2\,\mathrm{d}\mathbf{x} + \int_{B^+} |\,\mathbf{grad}\,\mathbf{w}(\mathbf{x})|^2\,\mathrm{d}\mathbf{x} + \int_{B^-} |\sum\nolimits_{j=1}^3 \lambda_j w^1(x_1,x_2,-\frac{x_3}{j})|^2\,\mathrm{d}\mathbf{x}\\ &\quad + \int_{B^-} |\sum\nolimits_{j=1}^3 \lambda_j w^2(x_1,x_2,-\frac{x_3}{j})|^2\,\mathrm{d}\mathbf{x} + \int_{B^-} |\sum\nolimits_{j=1}^3 \frac{\lambda_j}{-j} w^3(x_1,x_2,-\frac{x_3}{j})|^2\,\mathrm{d}\mathbf{x}\\ &\quad + \sum_{i=1}^3\sum_{k=1}^3 \int_{B^+} |w^i_{x_k}(\mathbf{x})|^2\,\mathrm{d}\mathbf{x} + \sum_{k=1}^3 \int_{B^-} |\sum\nolimits_{j=1}^3 \lambda_j w^1_{x_k}(x_1,x_2,-\frac{x_3}{j})|^2\,\mathrm{d}\mathbf{x}\\ &\quad + \sum_{k=1}^3 \int_{B^-} |\sum\nolimits_{j=1}^3 \lambda_j w^2_{x_k}(x_1,x_2,-\frac{x_3}{j})|^2\,\mathrm{d}\mathbf{x}\\ &\quad + \sum_{k=1}^3 \int_{B^-} |\sum\nolimits_{j=1}^3 \frac{\lambda_j}{-j} w^3_{x_k}(x_1,x_2,-\frac{x_3}{j})|^2\,\mathrm{d}\mathbf{x}\\ &\le C\left(\int_{B^+} |\mathbf{w}(\mathbf{x})|^2\,\mathrm{d}\mathbf{x} + \int_{B^+} |\,\mathbf{grad}\,\mathbf{w}(\mathbf{x})|^2\,\mathrm{d}\mathbf{x}\right).\end{aligned} \tag{3.7}$$

To show that $\|\mathbf{curl}\,\widetilde{\mathbf{w}}\|_{\boldsymbol{H}^1(B)} \le C\,\|\mathbf{curl}\,\mathbf{w}\|_{\boldsymbol{H}^1(B+)}$, we exploit the amazing symmetry in the following equality,

$$\begin{aligned}&\int_B |\,\mathbf{curl}\,\widetilde{\mathbf{w}}(\mathbf{x})|^2\,\mathrm{d}\mathbf{x}\\ &= \int_{B^+} |w^3_{x_2}(\mathbf{x}) - w^2_{x_3}(\mathbf{x})|^2\,\mathrm{d}\mathbf{x} + \int_{B^+} |w^1_{x_3}(\mathbf{x}) - w^3_{x_1}(\mathbf{x})|^2\,\mathrm{d}\mathbf{x} + \int_{B^+} |w^2_{x_1}(\mathbf{x}) - w^1_{x_2}(\mathbf{x})|^2\,\mathrm{d}\mathbf{x}\\ &\quad + \int_{B^-} |\sum\nolimits_{j=1}^3 \frac{\lambda_j}{-j} w^3_{x_2}(x_1,x_2,-\frac{x_3}{j}) - \sum\nolimits_{j=1}^3 \frac{\lambda_j}{-j} w^2_{x_3}(x_1,x_2,-\frac{x_3}{j})|^2\,\mathrm{d}\mathbf{x}\\ &\quad + \int_{B^-} |\sum\nolimits_{j=1}^3 \frac{\lambda_j}{-j} w^1_{x_3}(x_1,x_2,-\frac{x_3}{j}) - \sum\nolimits_{j=1}^3 \frac{\lambda_j}{-j} w^3_{x_1}(x_1,x_2,-\frac{x_3}{j})|^2\,\mathrm{d}\mathbf{x}\\ &\quad + \int_{B^-} |\sum\nolimits_{j=1}^3 \lambda_j w^2_{x_1}(x_1,x_2,-\frac{x_3}{j}) - \sum\nolimits_{j=1}^3 \lambda_j w^1_{x_2}(x_1,x_2,-\frac{x_3}{j})|^2\,\mathrm{d}\mathbf{x}\,.\end{aligned}$$

We see that the coefficients within the square terms of those integrations over B^- can be extracted as scaling factors. Then the same procedure of collecting coefficients and using the mirror reflection yields

$$\begin{aligned}&\int_B |\,\mathbf{curl}\,\widetilde{\mathbf{w}}(\mathbf{x})|^2\,\mathrm{d}\mathbf{x} + \int_B |\,\mathbf{grad}\,\mathbf{curl}\,\widetilde{\mathbf{w}}(\mathbf{x})|^2\,\mathrm{d}\mathbf{x}\\ &\qquad \le C\left(\int_{B^+} |\,\mathbf{grad}\,\mathbf{curl}\,\mathbf{w}(\mathbf{x})|^2\,\mathrm{d}\mathbf{x} + \int_{B^+} |\,\mathbf{curl}\,\mathbf{w}(\mathbf{x})|^2\,\mathrm{d}\mathbf{x}\right),\end{aligned}$$

which, together with (3.7), implies the continuity

$$\|\widetilde{\mathbf{w}}\|_{\boldsymbol{H}^1(\mathbf{curl};B)} \le C\,\|\mathbf{w}\|_{\boldsymbol{H}^1(\mathbf{curl};B^+)}\,, \tag{3.8}$$

where the constant C in (3.8) is a polynomial of at most second order in terms of λ_1, λ_2 and λ_3.

In case of ∂U being not necessarily flat near $\mathbf{x}^0$ we apply the usual flattening technique and partition of unity localization in order to reduce the situation to the one discussed above. □

For our purpose, a tailored version of Theorem 3.4 is the following corollary.

Corollary 3.5. *There exist two bounded linear operators for $i = 1, 2$, respectively*

$$\mathbf{E}^i_{\mathbf{curl}} \,:\, \boldsymbol{H}^1(\mathbf{curl};\Omega_i) \to \boldsymbol{H}^1(\mathbf{curl};\Omega) \tag{3.9}$$

such that for each $\mathbf{u} \in \boldsymbol{H}^1(\mathbf{curl};\Omega_i)$:

1. $\mathbf{E}^i_{\mathbf{curl}}\mathbf{u} = \mathbf{u}$ *a.e. in* Ω_i.
2. $\left\|\mathbf{E}^i_{\mathbf{curl}}\mathbf{u}\right\|_{\boldsymbol{H}^1(\mathbf{curl};\Omega)} \le C \left\|\mathbf{u}\right\|_{\boldsymbol{H}^1(\mathbf{curl};\Omega_i)}$, *with the constant C depending only on Ω.*

Proof. Noticing the fact that the interface Γ is at least C^2-smooth and some slight modifications of the proof of Theorem 3.4 yield the desired result. □

For the later use, we will need the following variant of the well-known trace inequality in a pyramid. The crucial fact is that the estimate in this inequality can be applied to a pyramid with slender bottom face.

Lemma 3.6. *Let P be a pyramid with F being its quadrilateral bottom face and O its apex (see Figure 4). Then we have*

$$\|u\|^2_{L^2(F)} \le \frac{3}{d}\|u\|_{L^2(P)}(h_P\|\mathbf{grad}\, u\|_{L^2(P)} + \|u\|_{L^2(P)}) \quad \forall u \in H^1(P)\,,$$

where $d := \mathrm{dist}(O, F)$, $h_P := \max\{|\mathbf{x}-\mathbf{y}| : \mathbf{x}, \mathbf{y} \in P\}$. Moreover, if $d \sim O(h_P)$ and $h_P < 1$, we have

$$\|u\|^2_{L^2(F)} \le C\left(\frac{1}{h_P}\|u\|^2_{L^2(P)} + \|\mathbf{grad}\, u\|^2_{L^2(P)}\right) \quad \forall u \in H^1(P)\,, \tag{3.10}$$

with $C > 0$ independent of h_P.

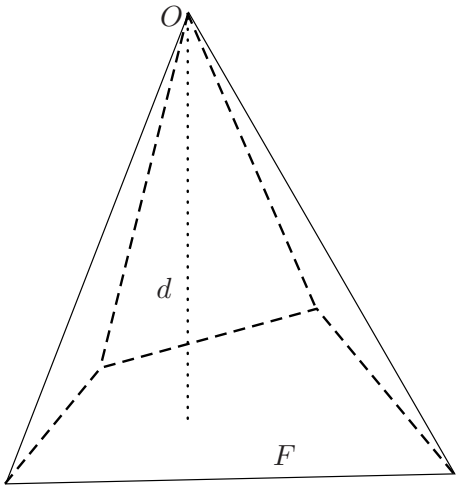

Figure 4: Sketch of the pyramid from Lemma 3.6.

Proof. Without loss of generality, we may assume that the apex O, possibly through simple translation, is the origin. Then it is obvious to see that

$$F \subset \{\mathbf{x} \mid \mathbf{x}\cdot\mathbf{n}_F = d\},$$

where $\mathbf{n}_F$ is the outward unit normal vector on the bottom side F. Making use of the fact that $\mathbf{x}\cdot\mathbf{n}$ vanishes on all the other sides of the pyramid except the bottom one, divergence law and Cauchy-Schwarz inequality yield

$$\begin{aligned}\int_F u^2 \mathrm{d}S &= \frac{1}{d}\int_{\partial P} u^2 \mathbf{x}\cdot\mathbf{n}\,\mathrm{d}S = \frac{1}{d}\int_P \mathrm{div}(u^2\mathbf{x})\mathrm{d}\mathbf{x}\\ &= \frac{1}{d}\int_P \left(2u\,\mathbf{grad}\,u\cdot\mathbf{x} + 3u^2\right)\mathrm{d}\mathbf{x}\\ &\le \frac{3}{d}\|u\|_{L^2(P)}\left(h_P\|\mathbf{grad}\,u\|_{L^2(P)} + \|u\|_{L^2(P)}\right),\end{aligned}$$

where $\mathbf{n}$ is the unit outward normal vector on ∂P.

If $d\sim O(h_P)$ and $h_P<1$, by the Cauchy-Schwarz inequality we have

$$\begin{aligned}\int_F u^2\mathrm{d}S &\le C\left(\|u\|_{L^2(P)}\|\mathbf{grad}\,u\|_{L^2(P)} + \frac{1}{h_P}\|u\|^2_{L^2(P)}\right)\\ &\le C\left(\|\mathbf{grad}\,u\|^2_{L^2(P)} + \frac{1}{h_P}\|u\|^2_{L^2(P)}\right).\end{aligned}$$

This completes the proof. □

4 Convergence analysis

In this section, we show the optimal convergence for the $\boldsymbol{H}(\mathbf{curl})$-elliptic interface problem (1.1)–(1.4) using the lowest order $\boldsymbol{H}(\mathbf{curl};\Omega)$-conforming finite element approximation. We will make use of a perturbation argument combined with the technical tools provided in Section 3.

First we show a technical lemma to be used for the main theorem on optimal convergence.

Lemma 4.1. *If* $\mathbf{u}\in \boldsymbol{H}_0(\mathbf{curl};\Omega)\cap\boldsymbol{H}^1(\mathbf{curl};\Omega_1)\cap\boldsymbol{H}^1(\mathbf{curl};\Omega_2)$, *then we have*

$$\sum_{K\in\mathcal{T}_*^1}\|\mathbf{E}^1_{\mathbf{curl}}\mathbf{u}_1\|^2_{\boldsymbol{H}(\mathbf{curl};K\cap\Omega_2)} \le \|\mathbf{E}^1_{\mathbf{curl}}\mathbf{u}_1\|^2_{\boldsymbol{H}(\mathbf{curl};S^2_\delta)} \le C\delta\|\mathbf{u}_1\|^2_{\boldsymbol{H}^1(\mathbf{curl};\Omega_1)}, \tag{4.1}$$

$$\sum_{K\in\mathcal{T}_*^1}\|\mathbf{u}_2\|^2_{\boldsymbol{H}(\mathbf{curl};K\cap\Omega_2)} \le \|\mathbf{u}_2\|^2_{\boldsymbol{H}(\mathbf{curl};S^2_\delta)} \le C\delta\|\mathbf{u}_2\|^2_{\boldsymbol{H}^1(\mathbf{curl};\Omega_2)}. \tag{4.2}$$

Analogously:

$$\sum_{K\in\mathcal{T}_*^2}\|\mathbf{E}^2_{\mathbf{curl}}\mathbf{u}_2\|^2_{\boldsymbol{H}(\mathbf{curl};K\cap\Omega_1)} \le \|\mathbf{E}^2_{\mathbf{curl}}\mathbf{u}_2\|^2_{\boldsymbol{H}(\mathbf{curl};S^1_\delta)} \le C\delta\|\mathbf{u}_2\|^2_{\boldsymbol{H}^1(\mathbf{curl};\Omega_2)}, \tag{4.3}$$

$$\sum_{K\in\mathcal{T}_*^2}\|\mathbf{u}_1\|^2_{\boldsymbol{H}(\mathbf{curl};K\cap\Omega_1)} \le \|\mathbf{u}_1\|^2_{\boldsymbol{H}(\mathbf{curl};S^1_\delta)} \le C\delta\|\mathbf{u}_1\|^2_{\boldsymbol{H}^1(\mathbf{curl};\Omega_1)}. \tag{4.4}$$

with the constant C depending only on the domain Ω, but independent of $\mathbf{u}$.

Proof. We only prove (4.1)–(4.2) since the estimates (4.3)–(4.4) are obtained from (4.1)–(4.2) by interchanging the subscripts 1 and 2. To see (4.1), we note $\cup_{K\in\mathcal{T}_*^1}K\cap\Omega_2\subset S^2_\delta$; furthermore, since all elements of $\mathcal{T}_h$ are pairwise disjoint, the first inequality in (4.1) follows immediately. For the second estimate, using the Corollary 3.2 and the continuity property of the extension operator $\mathbf{E}^1_{\mathbf{curl}}$ yields:

$$\|\mathbf{E}^1_{\mathbf{curl}}\mathbf{u}_1\|^2_{\boldsymbol{H}(\mathbf{curl};S^2_\delta)} \le C\delta\|\mathbf{E}^1_{\mathbf{curl}}\mathbf{u}_1\|^2_{\boldsymbol{H}^1(\mathbf{curl};\Omega_2)} \le C\delta\|\mathbf{u}_1\|^2_{\boldsymbol{H}^1(\mathbf{curl};\Omega_1)}.$$

The estimate (4.2) is obtained analogously by noting the fact that $\cup_{K\in\mathcal{T}_*^1}K\cap\Omega_2\subset S^2_\delta$. □

To obtain the convergence result, we need to show an appropriate interpolation error estimate for the interface-aware interpolation operator $\widetilde{\mathbf{I}}_h$ in Def. 2.7.

Lemma 4.2. *Assume* $\mathbf{u} \in \boldsymbol{H}_0(\mathbf{curl};\Omega) \cap \boldsymbol{H}^1(\mathbf{curl};\Omega_1) \cap \boldsymbol{H}^1(\mathbf{curl};\Omega_2)$*, Then we have the following error estimate under Assumptions 2.1 and 2.3:*

$$\left\|\mathbf{u} - \widetilde{\mathbf{I}}_h\mathbf{u}\right\|_{\boldsymbol{H}(\mathbf{curl};\Omega)} \leq C(h + \sqrt{\delta} + \frac{\delta}{\sqrt{h}}) \left(\|\mathbf{u}\|_{\boldsymbol{H}^1(\mathbf{curl};\Omega_1)} + \|\mathbf{u}\|_{\boldsymbol{H}^1(\mathbf{curl};\Omega_2)}\right) \tag{4.5}$$

with the constant C *depending only on the domain* Ω*, but independent of* $\mathbf{u}$ *and the meshsize* h*.*

Proof. Take any interface element $K \in \mathcal{T}_*^1$. We observe a crucial identity following from Definition 2.7 of the perturbed interpolation operator

$$\widetilde{\mathbf{I}}_h\mathbf{u}\Big|_K = \widetilde{\mathbf{I}}_h\mathbf{E}^1_{\mathbf{curl}}\mathbf{u}\Big|_K .$$

Thus we can always decompose the difference $\mathbf{u} - \widetilde{\mathbf{I}}_h\mathbf{u}$ over this interface element K into three parts:

$$\begin{aligned}\left(\mathbf{u} - \widetilde{\mathbf{I}}_h\mathbf{u}\right)\Big|_K = &\left(\mathbf{u} - \mathbf{E}^1_{\mathbf{curl}}\mathbf{u}\right)\Big|_K + \left(\mathbf{E}^1_{\mathbf{curl}}\mathbf{u} - \mathbf{I}_h\mathbf{E}^1_{\mathbf{curl}}\mathbf{u}\right)\Big|_K \\ &+ \left(\mathbf{I}_h\mathbf{E}^1_{\mathbf{curl}}\mathbf{u} - \widetilde{\mathbf{I}}_h\mathbf{E}^1_{\mathbf{curl}}\mathbf{u}\right)\Big|_K .\end{aligned} \tag{4.6}$$

Noting that $\mathbf{u} = \mathbf{E}^1_{\mathbf{curl}}\mathbf{u}$ on $K \cap \Omega_1$, then employing Lemma 4.1 and the continuity of $\mathbf{E}^1_{\mathbf{curl}}$ lead to the error estimate for the first term in (4.6):

$$\begin{aligned}\sum_{K\in\mathcal{T}_*^1} \left\|\mathbf{u} - \mathbf{E}^1_{\mathbf{curl}}\mathbf{u}\right\|^2_{\boldsymbol{H}(\mathbf{curl};K)} &\leq \sum_{K\in\mathcal{T}_*^1} \|\mathbf{u}\|^2_{\boldsymbol{H}(\mathbf{curl};K\cap\Omega_2)} + \sum_{K\in\mathcal{T}_*^1} \left\|\mathbf{E}^1_{\mathbf{curl}}\mathbf{u}\right\|^2_{\boldsymbol{H}(\mathbf{curl};K\cap\Omega_2)} \\ &\leq C\delta \left(\|\mathbf{u}\|^2_{\boldsymbol{H}^1(\mathbf{curl};\Omega_1)} + \|\mathbf{u}\|^2_{\boldsymbol{H}^1(\mathbf{curl};\Omega_2)}\right) .\end{aligned} \tag{4.7}$$

A classical interpolation result (cf. [25, Theorem 5.41]) of the standard interpolation operator $\mathbf{I}_h$ in view of Lemma 2.6 and the continuous property of $\mathbf{E}^1_{\mathbf{curl}}$ give

$$\begin{aligned}\sum_{K\in\mathcal{T}_*^1} \left\|\mathbf{E}^1_{\mathbf{curl}}\mathbf{u} - \mathbf{I}_h\mathbf{E}^1_{\mathbf{curl}}\mathbf{u}\right\|^2_{\boldsymbol{H}(\mathbf{curl};K)} &\leq C \sum_{K\in\mathcal{T}_*^1} h^2 \left\|\mathbf{E}^1_{\mathbf{curl}}\mathbf{u}\right\|^2_{\boldsymbol{H}^1(\mathbf{curl};K)} \\ &\leq Ch^2 \left\|\mathbf{E}^1_{\mathbf{curl}}\mathbf{u}\right\|^2_{\boldsymbol{H}^1(\mathbf{curl};\Omega)} \leq Ch^2 \|\mathbf{u}\|^2_{\boldsymbol{H}^1(\mathbf{curl};\Omega_1)} .\end{aligned} \tag{4.8}$$

For the third term on the right hand side of (4.6), we observe that the only difference between $\mathbf{I}_h\mathbf{E}^1_{\mathbf{curl}}\mathbf{u}$ and $\widetilde{\mathbf{I}}_h\mathbf{E}^1_{\mathbf{curl}}\mathbf{u}$ comes from their degrees of freedom endowed with the interface edges

which are immersed within the interface buffer region S_δ. We have

$$
\begin{aligned}
&\left\|\mathbf{I}_h\mathbf{E}^1_{\mathbf{curl}}\mathbf{u}-\widetilde{\mathbf{I}}_h\mathbf{E}^1_{\mathbf{curl}}\mathbf{u}\right\|^2_{\boldsymbol{H}(\mathbf{curl};K)}\\
\le\, & C\sum_{e\in\mathcal{E}_h\cap\overline{K}\cap S_\delta}\left(\left\|\left(\int_e\mathbf{E}^1_{\mathbf{curl}}\mathbf{u}\cdot\mathrm{d}\vec{s}-\int_{\widetilde{e}}\mathbf{E}^1_{\mathbf{curl}}\mathbf{u}\cdot\mathrm{d}\vec{s}\right)\mathbf{b}_e\right\|^2\right.\\
&\qquad\left.+\left\|\left(\int_e\mathbf{E}^1_{\mathbf{curl}}\mathbf{u}\cdot\mathrm{d}\vec{s}-\int_{\widetilde{e}}\mathbf{E}^1_{\mathbf{curl}}\mathbf{u}\cdot\mathrm{d}\vec{s}\right)\mathbf{curl}\,\mathbf{b}_e\right\|^2\right)\\
\le\, & C\sum_{e\in\mathcal{E}_h\cap\overline{K}\cap S_\delta}\left(\|\mathbf{b}_e\|^2+\|\mathbf{curl}\,\mathbf{b}_e\|^2\right)\left(\int_e\mathbf{E}^1_{\mathbf{curl}}\mathbf{u}\cdot\mathrm{d}\vec{s}-\int_{\widetilde{e}}\mathbf{E}^1_{\mathbf{curl}}\mathbf{u}\cdot\mathrm{d}\vec{s}\right)^2\\
\le\, & C\sum_{e\in\mathcal{E}_h\cap\overline{K}\cap S_\delta}(h+\frac{1}{h})\left(\int_e\mathbf{E}^1_{\mathbf{curl}}\mathbf{u}\cdot\mathrm{d}\vec{s}-\int_{\widetilde{e}}\mathbf{E}^1_{\mathbf{curl}}\mathbf{u}\cdot\mathrm{d}\vec{s}\right)^2\\
\le\, & C\sum_{e\in\mathcal{E}_h\cap\overline{K}\cap S_\delta}\frac{1}{h}\left(\int_{S_{e,\widetilde{e}}}\mathbf{curl}\,\mathbf{E}^1_{\mathbf{curl}}\mathbf{u}\cdot\mathrm{d}\vec{S}\right)^2\\
\le\, & C\sum_{e\in\mathcal{E}_h\cap\overline{K}\cap S_\delta}\frac{1}{h}|S_{e,\widetilde{e}}|\left(\int_{S_{e,\widetilde{e}}}|\,\mathbf{curl}\,\mathbf{E}^1_{\mathbf{curl}}\mathbf{u}|^2\mathrm{d}S\right)\\
\le\, & C\sum_{e\in\mathcal{E}_h\cap\overline{K}\cap S_\delta}\delta\left(\int_{S_{e,\widetilde{e}}}|\,\mathbf{curl}\,\mathbf{E}^1_{\mathbf{curl}}\mathbf{u}|^2\mathrm{d}S\right),
\end{aligned}
\tag{4.9}
$$

where we have employed estimates for edge element basis functions in the third inequality (cf. [25, Lemma. 5.43]), the Stokes theorem in the fourth inequality, and the Cauchy-Schwarz inequality in the fifth inequality. In the last inequality, $|S_{e,\widetilde{e}}|$ stands for the area of $S_{e,\widetilde{e}}$, which is of the order $h\delta$ in view of Assumption 2.3 and Remark 2.5.

We continue by estimating the last term in (4.9). For each piecewise planar surface $S_{e,\widetilde{e}}$, it can be embedded into a narrow region between the slim bottom sides of two pyramid-type elements P_1^e and P_2^e which share the same apex q and lie in two adjacent interface elements K_1^e and K_2^e, respectively, sharing the common interface edge e (see Figure 5). These pyramids P_1^e and P_2^e are taken to be so slender that they lie completely inside S_δ.

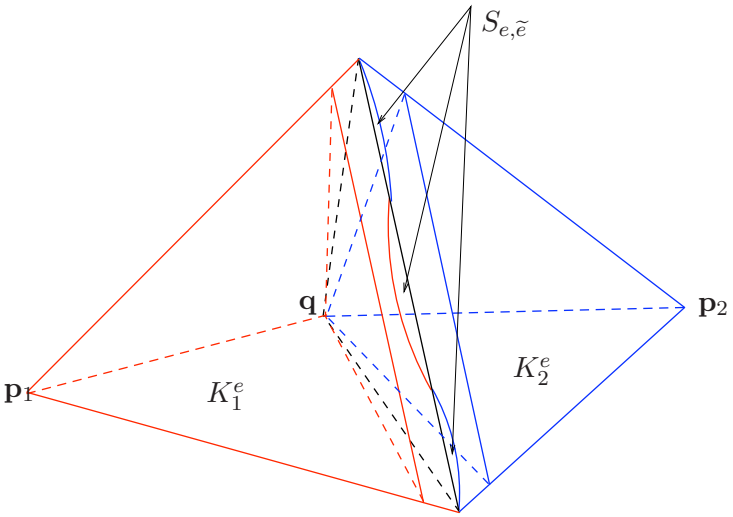

Figure 5: Piecewise planar surface $S_{e,\widetilde{e}}$ imbedded in pyramid-type elements P_1^e and P_2^e in two adjacent interface elements K_1^e and K_2^e.

Now by enlarging the area of the surface integral from $S_{e,\widetilde{e}}$ to be the two slender bottom sides of

those two pyramids P_1^e and P_2^e, observing that the height to the bottom sides of P_1^e and P_2^e are still of the order h, and applying Lemma 3.6, we arrive at

$$\int_{S_{e,\tilde{e}}} |\,\mathbf{curl}\,\mathbf{E}^1_{\mathbf{curl}}\mathbf{u}|^2 \mathrm{d}S \le C\left(\frac{1}{h}\left\|\mathbf{curl}\,\mathbf{E}^1_{\mathbf{curl}}\mathbf{u}\right\|^2_{\boldsymbol{L}^2(P_1^e\cup P_2^e)} + \left\|\mathbf{grad}\,\mathbf{curl}\,\mathbf{E}^1_{\mathbf{curl}}\mathbf{u}\right\|^2_{\boldsymbol{L}^2(P_1^e\cup P_2^e)}\right). \tag{4.10}$$

Plugging (4.10) into (4.9), and summing over all K in $\mathcal{T}^1_*$ give us

$$\begin{aligned}
&\sum_{K\in\mathcal{T}^1_*}\left\|\mathbf{I}_h\mathbf{E}^1_{\mathbf{curl}}\mathbf{u}-\widetilde{\mathbf{I}}_h\mathbf{E}^1_{\mathbf{curl}}\mathbf{u}\right\|^2_{\boldsymbol{H}(\mathbf{curl};K)}\\
&\le C\sum_{K\in\mathcal{T}^1_*}\sum_{e\in\mathcal{E}_h\cap\overline{K}\cap S_\delta}\left(\frac{\delta}{h}\left\|\mathbf{curl}\,\mathbf{E}^1_{\mathbf{curl}}\mathbf{u}\right\|^2_{\boldsymbol{L}^2(P_1^e\cup P_2^e)}+\delta\left\|\mathbf{grad}\,\mathbf{curl}\,\mathbf{E}^1_{\mathbf{curl}}\mathbf{u}\right\|^2_{\boldsymbol{L}^2(P_1^e\cup P_2^e)}\right)\\
&\le C\left(\frac{\delta}{h}\left\|\mathbf{curl}\,\mathbf{E}^1_{\mathbf{curl}}\mathbf{u}\right\|^2_{\boldsymbol{L}^2(S_\delta)}+\delta\left\|\mathbf{grad}\,\mathbf{curl}\,\mathbf{E}^1_{\mathbf{curl}}\mathbf{u}\right\|^2_{\boldsymbol{L}^2(S_\delta)}\right)\\
&\le C(\frac{\delta^2}{h}+\delta)\left\|\mathbf{curl}\,\mathbf{E}^1_{\mathbf{curl}}\mathbf{u}\right\|^2_{\boldsymbol{H}^1(\Omega)}\\
&\le C(\frac{\delta^2}{h}+\delta)\left\|\mathbf{u}\right\|^2_{\boldsymbol{H}^1(\mathbf{curl};\Omega_1)}\ .
\end{aligned} \tag{4.11}$$

In the second inequality we have used the fact that

$$\bigcup_{K\in\mathcal{T}^1_*}\ \bigcup_{e\in\mathcal{E}_h\cap\overline{K}\cap S_\delta}(P_1^e\cup P_2^e)\subset S_\delta\,,$$

and that, thanks to the quasi-uniformity assumption on the triangulation, there is only finite overlap among those slim pyramids sharing a common interface edges. In the third inequality we have employed Lemma 3.1 for the first term, and the continuity of $\mathbf{E}^1_{\mathbf{curl}}$ in the last inequality.

In the next step, for any non-interface $K\in\mathcal{T}^1$, we see that $\widetilde{\mathbf{I}}_h\mathbf{u}$ and $\mathbf{I}_h\mathbf{u}$ are identical for $\mathbf{u}\in\boldsymbol{H}^1(\mathbf{curl};K)$. Thus a classical interpolation approximation (cf. [25, Theorem 5.41]) yields

$$\begin{aligned}
\sum_{K\in\mathcal{T}^1}\left\|\mathbf{u}-\widetilde{\mathbf{I}}_h\mathbf{u}\right\|^2_{\boldsymbol{H}(\mathbf{curl};K)} &= \sum_{K\in\mathcal{T}^1}\left\|\mathbf{u}-\mathbf{I}_h\mathbf{u}\right\|^2_{\boldsymbol{H}(\mathbf{curl};K)}\\
\le C\sum_{K\in\mathcal{T}^1}h^2\left\|\mathbf{u}\right\|^2_{\boldsymbol{H}^1(\mathbf{curl};K)} &\le Ch^2\left\|\mathbf{u}\right\|^2_{\boldsymbol{H}^1(\mathbf{curl};\Omega_1)}\ .
\end{aligned} \tag{4.12}$$

Combining (4.6), (4.7), (4.8), (4.11), and (4.12) yields

$$\sum_{K\in\mathcal{T}^1\cup\mathcal{T}^1_*}\left\|\mathbf{u}-\widetilde{\mathbf{I}}_h\mathbf{u}\right\|^2_{\boldsymbol{H}(\mathbf{curl};K)}\le C(\frac{\delta^2}{h}+\delta+h^2)\left(\left\|\mathbf{u}\right\|^2_{\boldsymbol{H}^1(\mathbf{curl};\Omega_1)}+\left\|\mathbf{u}\right\|^2_{\boldsymbol{H}^1(\mathbf{curl};\Omega_2)}\right). \tag{4.13}$$

In a completely analogous manner, we can repeat the previous arguments by interchanging the indices from 1 to 2 and arrive at

$$\sum_{K\in\mathcal{T}^2\cup\mathcal{T}^2_*}\left\|\mathbf{u}-\widetilde{\mathbf{I}}_h\mathbf{u}\right\|^2_{\boldsymbol{H}(\mathbf{curl};K)}\le C(\frac{\delta^2}{h}+\delta+h^2)\left(\left\|\mathbf{u}\right\|^2_{\boldsymbol{H}^1(\mathbf{curl};\Omega_1)}+\left\|\mathbf{u}\right\|^2_{\boldsymbol{H}^1(\mathbf{curl};\Omega_2)}\right). \tag{4.14}$$

Combining (4.13) and (4.14) yields the desired approximation property and thus completes the proof.

□

Now we are in a position to state our main theorem about the optimal convergence of edge element Galerkin solutions of $\boldsymbol{H}(\mathbf{curl})$-elliptic interface problems.

Theorem 4.3. *Let* $\mathbf{u}$ *and* $\mathbf{u}_h$ *be the solutions to problems* $(\mathbf{P})$ *and* $(\widetilde{\mathbf{P}}_h)$*, respectively, and assume* $\mathbf{u} \in \boldsymbol{H}_0(\mathbf{curl};\Omega) \cap \boldsymbol{H}^1(\mathbf{curl};\Omega_1) \cap \boldsymbol{H}^1(\mathbf{curl};\Omega_2)$*. Then we have the following error estimate under Assumptions 2.1 and 2.3:*

$$\|\mathbf{u}-\mathbf{u}_h\|_{\boldsymbol{H}(\mathbf{curl};\Omega)} \leq Ch(\|\mathbf{u}\|_{\boldsymbol{H}^1(\mathbf{curl};\Omega_1)} + \|\mathbf{u}\|_{\boldsymbol{H}^1(\mathbf{curl};\Omega_2)}) \tag{4.15}$$

with the constant $C > 0$ *independent of* $\mathbf{u}$ *and the meshsize* h*.*

Proof. By the first Strang lemma (see, e.g., [12], Theorem 4.1.1) appliedd to (2.6) and (2.8)

$$\|\mathbf{u}-\mathbf{u}_h\|_{\boldsymbol{H}(\mathbf{curl};\Omega)} \leq C \inf_{\mathbf{w}_h\in\mathbf{E}_h} \left\{ \|\mathbf{u}-\mathbf{w}_h\|_{\boldsymbol{H}(\mathbf{curl};\Omega)} + \sup_{\mathbf{v}_h\in\mathbf{E}_h} \frac{|a(\mathbf{w}_h,\mathbf{v}_h)-a_h(\mathbf{w}_h,\mathbf{v}_h)|}{\|\mathbf{v}_h\|_{\boldsymbol{H}(\mathbf{curl};\Omega)}} \right\}. \tag{4.16}$$

In particular, we choose $\mathbf{w}_h = \widetilde{\mathbf{I}}_h\mathbf{u}$. By Lemma 4.2 we have

$$\|\mathbf{u}-\widetilde{\mathbf{I}}_h\mathbf{u}\|_{\boldsymbol{H}(\mathbf{curl};\Omega)} \leq C(\frac{\delta}{\sqrt{h}} + h + \sqrt{\delta}) \left(\|\mathbf{u}\|_{\boldsymbol{H}^1(\mathbf{curl};\Omega_1)} + \|\mathbf{u}\|_{\boldsymbol{H}^1(\mathbf{curl};\Omega_2)} \right). \tag{4.17}$$

Next, for any $\mathbf{v}_h \in \mathbf{E}_h$ we can derive by using Lemma 4.1 and Corollary 3.2 that

$$\begin{aligned} |a^{\Delta}(\widetilde{\mathbf{I}}_h\mathbf{u},\mathbf{v}_h)| &\leq C \quad \|\widetilde{\mathbf{I}}_h\mathbf{u}\|_{\boldsymbol{H}(\mathbf{curl};S_\delta)} \|\mathbf{v}_h\|_{\boldsymbol{H}(\mathbf{curl};S_\delta)} \\ &\leq C \quad \left(\|\mathbf{u}\|_{\boldsymbol{H}(\mathbf{curl};S_\delta)} + \|\mathbf{u}-\widetilde{\mathbf{I}}_h\mathbf{u}\|_{\boldsymbol{H}(\mathbf{curl};S_\delta)} \right) \|\mathbf{v}_h\|_{\boldsymbol{H}(\mathbf{curl};S_\delta)} \\ &\leq C \quad (\sqrt{\delta} + h + \frac{\delta}{\sqrt{h}}) \left(\|\mathbf{u}\|_{\boldsymbol{H}^1(\mathbf{curl};\Omega_1)} + \|\mathbf{u}\|_{\boldsymbol{H}^1(\mathbf{curl};\Omega_2)} \right) \|\mathbf{v}_h\|_{\boldsymbol{H}(\mathbf{curl};\Omega)}, \end{aligned}$$

which implies that

$$\sup_{v\in S^{p,1}(\mathcal{T})} \frac{|a^{\Delta}(\widetilde{\mathbf{I}}_h\mathbf{u},\mathbf{v}_h)|}{\|\mathbf{v}_h\|_{\boldsymbol{H}(\mathbf{curl};\Omega)}} \leq C(\sqrt{\delta} + h + \frac{\delta}{\sqrt{h}}) \left(\|\mathbf{u}\|_{\boldsymbol{H}^1(\mathbf{curl};\Omega_1)} + \|\mathbf{u}\|_{\boldsymbol{H}^1(\mathbf{curl};\Omega_2)} \right). \tag{4.18}$$

The desired estimate now follows from Assumption 2.3 by substituting $\delta \sim \mathscr{O}(h^2)$ into wherever δ occurs in (4.16)-(4.18) and plugging (4.17)-(4.18) into (4.16). □

In addition, it is possible to relax the regularity of the global solution $\mathbf{u}$ in Theorem 4.3 and require only $\mathbf{u} \in \boldsymbol{H}_0(\mathbf{curl};\Omega) \cap \boldsymbol{H}^s(\mathbf{curl};\Omega_1) \cap \boldsymbol{H}^s(\mathbf{curl};\Omega_2)$ for $0 \leq s \leq 1$. The interpolation arguments yield the following optimal s-order of convergence with techniques of interpolation spaces (see, e.g., [4] or [24, Theorem B.2]).

Theorem 4.4. *Let* $\mathbf{u}$ *and* $\mathbf{u}_h$ *be the solutions to problems* $(\mathbf{P})$ *and* $(\widetilde{\mathbf{P}}_h)$*, respectively, and assume* $\mathbf{u} \in \boldsymbol{H}_0(\mathbf{curl};\Omega) \cap \boldsymbol{H}^s(\mathbf{curl};\Omega_1) \cap \boldsymbol{H}^s(\mathbf{curl};\Omega_2)$ *for* $0 \leq s \leq 1$*. Then we have the following error estimate under Assumptions 2.1 and 2.3:*

$$\|\mathbf{u}-\mathbf{u}_h\|_{\boldsymbol{H}(\mathbf{curl};\Omega)} \leq Ch^s(\|\mathbf{u}\|_{\boldsymbol{H}^s(\mathbf{curl};\Omega_1)} + \|\mathbf{u}\|_{\boldsymbol{H}^s(\mathbf{curl};\Omega_2)}). \tag{4.19}$$

with the constant $C > 0$ *independent of* $\mathbf{u}$ *and the meshsize* h*.*

Proof. Utilizing the following stability result from the Galerkin projection

$$\|\mathbf{u}-\mathbf{u}_h\|_{\boldsymbol{H}(\mathbf{curl};\Omega)} \leq C \|\mathbf{u}\|_{\boldsymbol{H}(\mathbf{curl};\Omega)}, \tag{4.20}$$

the convergence result (4.15) in Theorem 4.3, and the characterization of $\boldsymbol{H}^s(\mathbf{curl};\Omega)$ as interpolation space $\left[\boldsymbol{H}(\mathbf{curl};\Omega), \boldsymbol{H}^1(\mathbf{curl};\Omega) \right]_s$, see [19], we can achieve the desired result by interpolation. □

5 Numerical experiments

In this section, we present two numerical examples to verify the theoretical prediction of the convergence analysis developed in previous sections. Our numerical experiments are implemented using MATLAB combined with the commercial package FEMLAB. We will test the first family of Nédélec elements of the lowest order. Note that after each step of mesh refinement, some regularly refined interface elements have to be slightly adjusted to meet the interface-aligned condition[1]. In the sequel, we will test the convergence rates for the relative error in the $\boldsymbol{H}(\mathbf{curl};\Omega)$-norm which is defined by

$$\text{Relative error} := \frac{\|\mathbf{u}-\mathbf{u}_h\|_{\boldsymbol{H}(\mathbf{curl};\Omega)}}{\|\mathbf{u}\|_{\boldsymbol{H}(\mathbf{curl};\Omega)}}, \tag{5.1}$$

and relative error in the energy norm, namely,

$$\text{Relative energy error} := \frac{\|\mathbf{u}-\mathbf{u}_h\|_a}{\|\mathbf{u}\|_a}. \tag{5.2}$$

Note that both $\boldsymbol{H}(\mathbf{curl};\Omega)$ and energy norms are numerically computed using a fourth order quadrature rule.

Example 5.1. Although the first example is two-dimensional, we remark that this 2D model problem using surface curl and planar curl operators fully captures all essential features of the 3D problem. The computational domain is a circular disk $\Omega = \{(x,y);\ x^2+y^2 \le r_2\}$, and the interface Γ is the unit circle $\{(x,y);\ x^2+y^2 = r_1\}$. The exact solution $\mathbf{u}(x,y)$ is given by

$$\mathbf{u}(x,y) = \begin{cases} \begin{pmatrix} \dfrac{x - n_1(r_1 - x^2 - y^2)y}{\chi_1} \\ \dfrac{-n_1(r_1 - x^2 - y^2)x + y}{\chi_1} \end{pmatrix}, & \text{if } x^2+y^2 \le r_1; \\ \begin{pmatrix} \dfrac{x - n_2(r_2 - x^2 - y^2)(r_1 - x^2 - y^2)y}{\chi_2} \\ \dfrac{-n_2(r_2 - x^2 - y^2)(r_1 - x^2 - y^2)x + y}{\chi_2} \end{pmatrix}, & \text{if } r_1 < x^2+y^2 \le r_2\,. \end{cases} \tag{5.3}$$

The solution has vanishing boundary condition and interface jump conditions. Here we choose $\beta = 1$, $\chi_1 = 1$, $\chi_2 = 10$, $r_1 = 0.6$, $r_2 = 1$, $n_2 = 20$, $n_1 = n_2(r_2^2 - r_1^2)$ and define the source functions $\mathbf{f}$ through the equation (1.1) using the exact solution defined in (5.3). Numerical convergence tests have been conducted to analyze the rates of the error decay.

In Figure 6 (a), the exact solution using scaled arrow flow is plotted for illustration. To the right, we can clearly see that the first family of edge elements of lowest order yields the optimal first order convergence in the $\boldsymbol{H}(\mathbf{curl};\Omega)$ norm from Figure 6 (b), which verifies what the theory predicted. For further verification, we increase the relative jump of the coefficients χ_2/χ_1 to 1000 and then decrease it to be 0.001, respectively, it is clear from Figure 6 (c) and Figure 6 (d) that the convergence rates are not affected by the extremely large or small relative jump.

Next we numerically investigate the relation between the relative error in the $\boldsymbol{H}(\mathbf{curl};\Omega)$-norm and relative jump of the coefficients χ_2/χ_1 as we refine the meshes. From Table 1, we can see that the relative error increases mildly as the magnitude of the relative jump do on the finer levels of triangulation.

Furthermore, we test the relation between the relative error in the energy norm and relative jump of the coefficients χ_2/χ_1. On a typical fine mesh with meshsize $h = 0.005$, we increase the relative jump of coefficients from 10^{-8} to 10^8 and plot the corresponding relative energy error in Figure 7, It can be seen that the curve of the relative energy error does not blow up except a small bump in case that the interior and outer coefficients matches each other in magnitude. This shows an advantage of our finite element method that it is quite robust with respect to the jump ratios of coefficients in terms of the energy norm, which sounds a good news for engineering and industrial practice.

[1] A simple way is done automatically by calling functions like `initmesh` and `refinemesh` in MATLAB's PDE toolbox or using the routines `distmesh2d` and `distmeshnd` developed by P.-O. Persson [27].

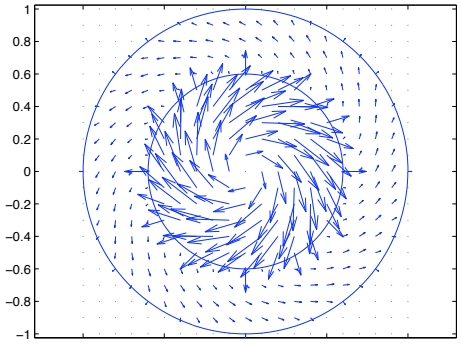

(a)

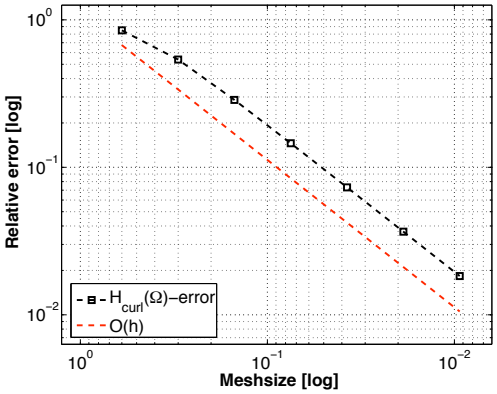

(b)

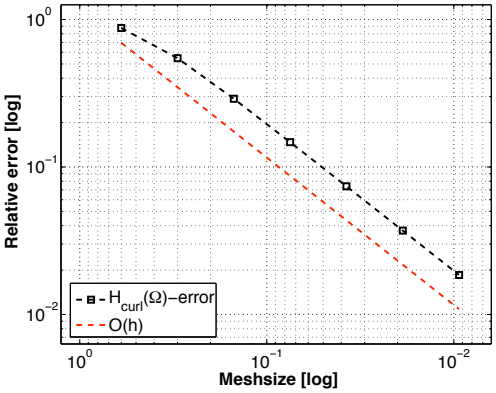

(c)

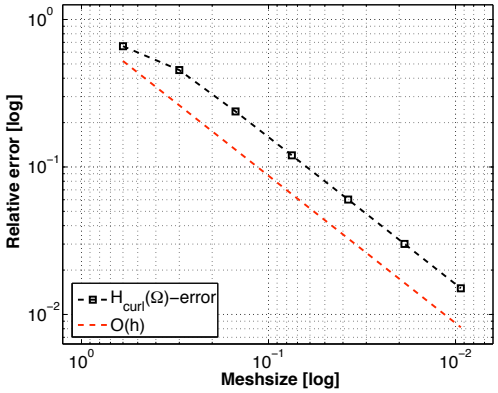

(d)

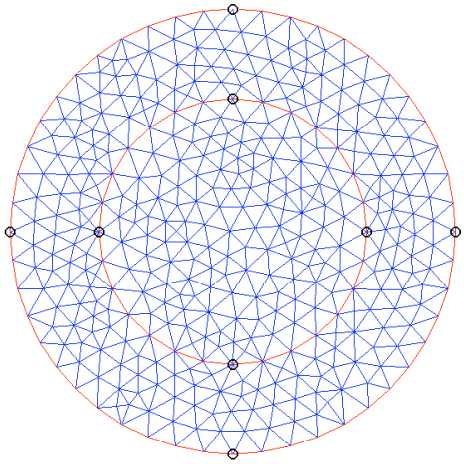

(e)

Figure 6: (a): The exact solution in Example 5.1 when $\chi_1 = 1$, $\chi_2 = 10$; (b): The convergence rate when $\chi_1 = 1$, $\chi_2 = 10$; (c): The convergence rate when $\chi_1 = 1$, $\chi_2 = 1000$; (d): The convergence rate when $\chi_1 = 1$, $\chi_2 = 0.001$; (e): A sample triangulation of interface-aligned mesh for Example 1 in 2D.

	Level of refinement						
χ_2/χ_1	1	2	3	4	5	6	7
10^{-3}	0.6591	0.4541	0.2380	0.1200	0.0601	0.0301	0.0150
10^{-2}	0.6196	0.4337	0.2338	0.1194	0.0600	0.0301	0.0150
10^{-1}	0.6050	0.4318	0.2336	0.1194	0.0601	0.0301	0.0150
10^{0}	0.6293	0.4458	0.2410	0.1231	0.0619	0.0310	0.0155
10^{1}	0.8485	0.5384	0.2865	0.1456	0.0731	0.0366	0.0183
10^{2}	0.8739	0.5464	0.2900	0.1473	0.0740	0.0370	0.0185
10^{3}	0.8755	0.5467	0.2901	0.1474	0.0740	0.0370	0.0185

Table 1: Relative error in the $\boldsymbol{H}(\mathbf{curl};\Omega)$-norm versus relative jump of coefficients at different levels of refinement.

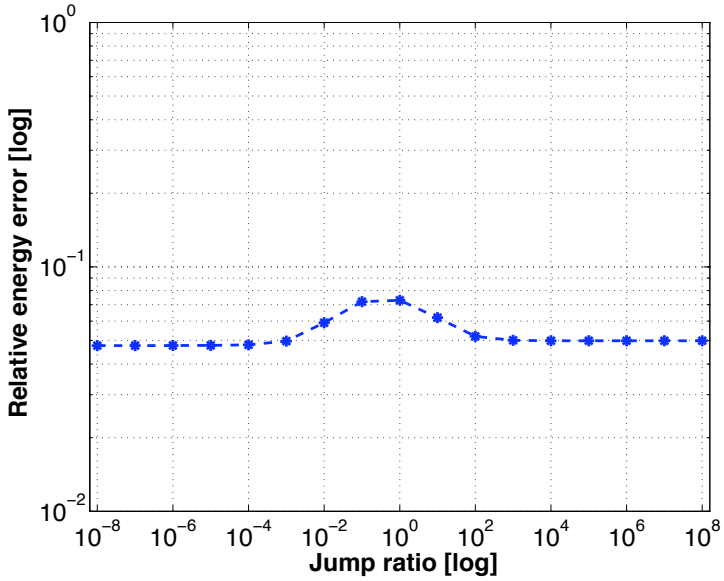

Figure 7: Relative error in the energy norm versus relative jump of coefficients for a fine triangulation with meshsize $h = 0.005$.

Example 5.2. The second example is a three-dimensional one. The computational domain is taken to be a ball $\Omega = \{(x, y, z);\ x^2+y^2+z^2 \le r_2\}$, and the interface Γ is a spherical surface $\{(x, y, z);\ x^2+y^2+z^2 = r_1\}$. The exact solution $\mathbf{u}(x, y, z)$ is given by

$$\mathbf{u}(x,y,z) = \begin{cases} \dfrac{1}{\chi_1}\mathbf{u}_1(x,y,z), & \text{if } x^2+y^2+z^2 \le r_1\,; \\ \dfrac{1}{\chi_2}\mathbf{u}_2(x,y,z), & \text{if } r_1 < x^2+y^2+z^2 \le r_2\,, \end{cases} \tag{5.4}$$

where $\mathbf{u}_1(x, y, z)$ is given by

$$\begin{pmatrix} x - n_1(r_1 - x^2 - y^2)y + n_1(r_1 - x^2 - y^2)z \\ -n_1(r_1 - x^2 - y^2)x + y - n_1(r_1 - x^2 - y^2)z \\ n_1(r_1 - x^2 - y^2)x - n_1(r_1 - x^2 - y^2)y + z \end{pmatrix}$$

and $\mathbf{u}_2(x, y, z)$ by

$$\begin{pmatrix} x - n_2(r_1 - x^2 - y^2)(r_2 - x^2 - y^2)y + n_2(r_1 - x^2 - y^2)(r_2 - x^2 - y^2)z \\ -n_2(r_1 - x^2 - y^2)(r_2 - x^2 - y^2)x + y + n_2(r_1 - x^2 - y^2)(r_2 - x^2 - y^2)z \\ n_2(r_1 - x^2 - y^2)(r_2 - x^2 - y^2)x - n_2(r_1 - x^2 - y^2)(r_2 - x^2 - y^2)y + z \end{pmatrix}$$

For this example, we choose $\beta = 1$, $\chi_1 = 1$, $\chi_2 = 0.1$, $r_1 = 1$, $r_2 = 2$, $n_2 = 20$, $n_1 = n_2(r_2^2 - r_1^2)$ and derive the source functions $\mathbf{f}$ through the equation (1.1) using the exact solution (5.4) which satisfies the homogeneous boundary condition and jump conditions on the interface. Numerical convergence tests are carried out to analyze the rates of the error decay using lowest order edge elements of the first family. We start our tests on a rather coarse mesh with mesh size $h = 1.2968$ and then refine the mesh in a regular and uniform way which subdivides a coarse element into eight smaller ones. The refinement process will be done for four consecutive times which amounts to around 2.5 million degrees of freedom at the finest mesh with mesh size $h = 0.0811$.

The exact solution are shown in Figure 8 (a). In Figure 8 (b), it can be clearly seen that as the mesh gets finer and finer, the line of the convergence rate tends to be parallel to the reference line of first order convergence in terms of the maximum meshsize. More precisely, in the asymptotic sense, edge elements indeed yield the optimal first order convergence in the $\boldsymbol{H}(\mathbf{curl}; \Omega)$ norm as predicted by theory. Next, as previously tested in Example 5.1 we adjust the relative jump of the coefficients χ_2/χ_1 to be 1000 and 0.001, respectively, and also plot the corresponding convergence rates in Figure 8 (c) and Figure 8 (d). Similar observations with asymptotic tendency of first order convergence rate with respect to the meshsize further consolidate our theoretical result.

In addition, we numerically check the relation between the relative error and relative jump of the coefficients χ_2/χ_1 as in Example 5.1. As can be seen from Table 2, the relative error in the $\boldsymbol{H}(\mathbf{curl}; \Omega)$-norm does not fluctuate wildly as we refine the meshes.

	Level of refinement				
χ_2/χ_1	1	2	3	4	5
10^{-3}	0.7763	0.6122	0.3481	0.1676	0.0791
10^{-2}	0.7263	0.5222	0.2810	0.1418	0.0709
10^{-1}	0.6628	0.4912	0.2736	0.1405	0.0707
10^{0}	0.6587	0.4915	0.2742	0.1408	0.0708
10^{1}	0.7948	0.5451	0.2974	0.1522	0.0767
10^{2}	0.8616	0.5718	0.3088	0.1578	0.0795
10^{3}	0.8635	0.5724	0.3090	0.1579	0.0795

Table 2: Relative error in the $\boldsymbol{H}(\mathbf{curl}; \Omega)$-norm versus relative jump of coefficients at different levels of refinement.

Last, we test the relation between the relative error in the energy norm and relative jump of the coefficients χ_2/χ_1. On a typical fine mesh with meshsize $h = 0.04$, we increase the relative jump

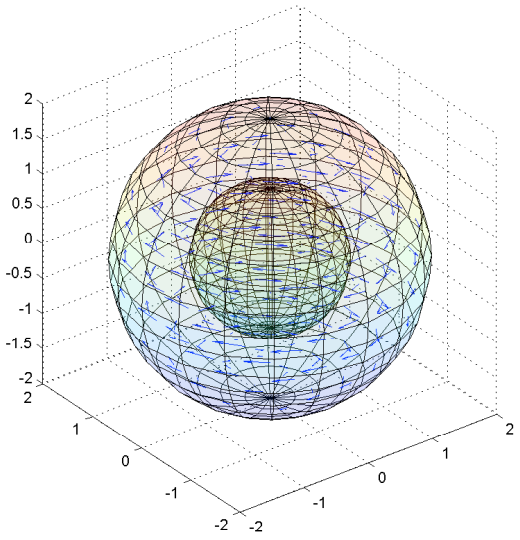

(a)

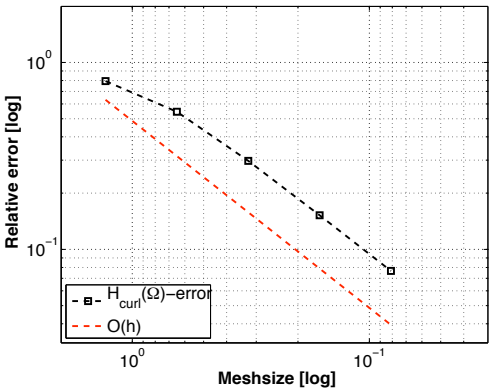

(b)

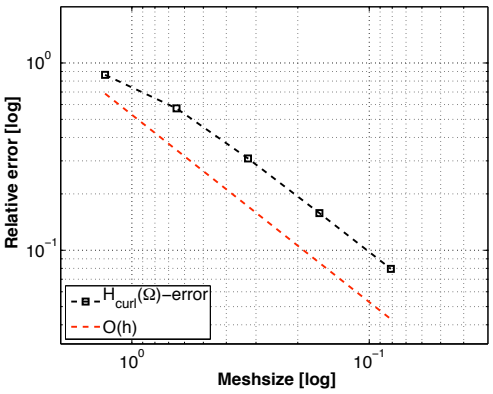

(c)

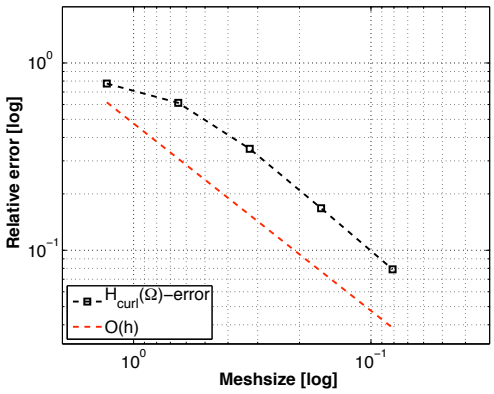

(d)

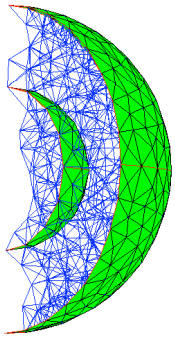

(e)

Figure 8: (a): The exact solution in Example 5.2 when $\chi_1 = 1$, $\chi_2 = 0.1$; (b): The convergence rate when $\chi_1 = 1$, $\chi_2 = 0.1$; (c): The convergence rate when $\chi_1 = 1$, $\chi_2 = 1000$; (d): The convergence rate when $\chi_1 = 1$, $\chi_2 = 0.001$; (e): A sample slice view of the triangulation of interface-aligned mesh for Example 2 in 3D.

of coefficients from 10^{-8} to 10^{8} and plot the corresponding relative energy error curve versus the relative jump in Figure 7, It can be seen that the numerical solution converges quite robustly in the sense of energy norm with respect to the relative jump of coefficients as in the first example.

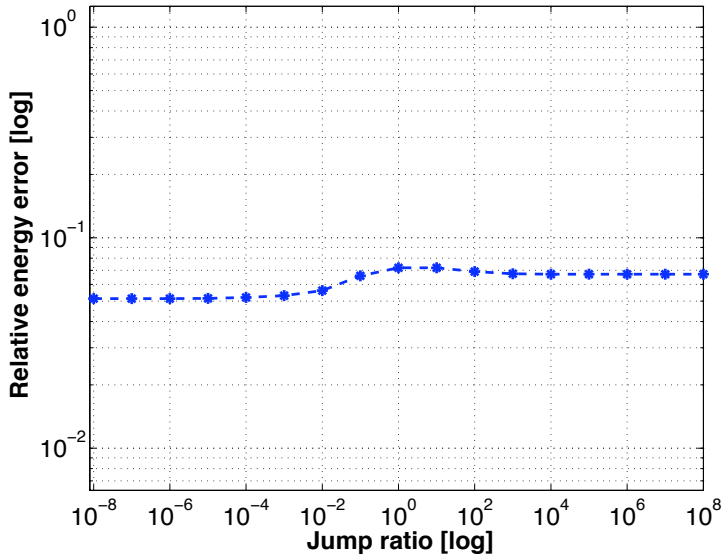

Figure 9: Relative error in the energy norm versus relative jump of coefficients for a fine triangulation with meshsize $h = 0.04$.

6 Conclusion

We have analyzed the convergence of the $\boldsymbol{H}(\mathbf{curl};\Omega)$-conforming finite element method for $\boldsymbol{H}(\mathbf{curl};\Omega)$-elliptic interface problems based on a family of interface-aligned meshes. The difficulty mainly arises from the discontinuity of the magnetic susceptibility coefficient χ in the $\mathbf{curl}\,\chi\,\mathbf{curl}$ term. It is pointed out that the analysis framework here can be generalized naturally to cover the case when the coefficient β in the low order term also has jumps across the interface, which may be due to the different conductivity of several materials. Optimal convergence results in $\boldsymbol{H}(\mathbf{curl};\Omega)$-norm are obtained under reasonable regularity assumptions. Further work may target the time-dependent $\boldsymbol{H}(\mathbf{curl};\Omega)$-interface problem and $\boldsymbol{H}(\mathrm{div};\Omega)$-elliptic interface problem.

References

[1] R. A. ADAMS, *Sobolev Spaces*, Academic Press, New York-London, 1975.

[2] H. AMMARI, A. BUFFA, AND J.-C. NÉDÉLEC, *A justification of eddy currents model for the Maxwell equations.*, SIAM J. Appl. Math., 60 (2000), pp. 1805–1823.

[3] J. W. BARRETT AND C. M. ELLIOTT, *Fitted and unfitted finite-element methods for elliptic equations with smooth interfaces*, IMA J. Numer. Anal., 7 (1987), pp. 283–300.

[4] J. BERGH AND J. LOFSTROM, *Interpolation Spaces*, Springer-Verlag, 1976.

[5] A. BOSSAVIT, *Two dual formulations of the 3D eddy–currents problem*, COMPEL, 4 (1985), pp. 103–116.

[6] A. BOSSAVIT, *Solving Maxwell's equations in a closed cavity and the question of spurious modes.*, IEEE Trans. Mag., 26 (1990), pp. 702–705.

[7] J. H. BRAMBLE AND J. T. KING., *A finite element method for interface problems in domains with smooth boundaries and interfaces*, Adv. Comput. Math., 6 (1996), pp. 109–138.

[8] S. C. BRENNER AND L. R. SCOTT, *The Mathematical Theory of Finite Element Methods*, Springer-Verlag, 2nd ed., 2005.

[9] E. BURMAN AND P. HANSBO, *Interior penalty stabilized lagrange multiplier methods for the finite element solution of elliptic interface problems*, to appear in IMA J. of Numer. Anal.

[10] T. CHAN AND J. ZOU, *A convergence theory of multilevel additive schwarz methods on unstructured meshes*, Numer. Algorithms, 13 (1996), pp. 365–398.

[11] Z. CHEN AND J. ZOU, *Finite element methods and their convergence for elliptic and parabolic interface problems*, Numer. Math., 79 (1998), pp. 175–202.

[12] P. G. CIARLET, *The Finite Element Method for Elliptic Problems*, Studies in Mathematics and its Applications, North-Holland Pub. Co., Amsterdam, New York, 1 ed., 1978.

[13] M. COSTABEL, M. DAUGE, AND S. NICAISE, *Singularities of Maxwell interface problems*, M2AN Math. Model. Numer. Anal., 33 (1999), pp. 627–649.

[14] H. DIRKS, *Qausi-stationary fields for microeletronic applications.*, Eletrical Engineering,, 79 (1996), pp. 145–155.

[15] L. C. EVANS, *Partial Differential Equations*, American Mathematical Society, Providence, Rhode Island, 1998.

[16] V. GIRAULT AND P. RAVIART, *Finite Element Methods for Navier-Stokes Equations*, Springer, Berlin, 1986.

[17] A. HANSBO AND P. HANSBO, *An unfitted finite element method, based on Nitsche's method, for elliptic interface problems*, Comput Methods Appl Mech Eng, 191 (2002), p. 5537?552.

[18] R. HIPTMAIR, *Finite elements in computational electromagnetism*, Acta Numerica, 11 (2002), pp. 237–339.

[19] R. HIPTMAIR, J. LI, AND J. ZOU, *Chracterization of* $\mathbf{H}^s(\mathbf{curl}, \Omega)$ *by Real Interpolation*, Tech. Report 2009-05, SAM, D-MATH, ETH, Zurich, Switzerland, 2009.

[20] R. HIPTMAIR, J. LI, AND J. ZOU, *Universal Extension for Sobolev Spaces of Differential Forms and Applications*, Tech. Report 2009-06, SAM, D-MATH, ETH, Zurich, Switzerland, 2009.

[21] J. HUANG AND J. ZOU, *A mortar element method for elliptic problems with discontinuous coefficients*, IMA J Numer. Anal., 22 (2002), pp. 549–576.

[22] J. LI, J. M. MELENK, B. WOHLMUTH, AND J. ZOU, *Convergence analysis of higher order finite element methods for elliptic interface problems*, Tech. Report, Institut für Analysis und Scientific Computing, Technische Universität Wien, Austria, 2008.

[23] Z. LI AND K. ITO, *The immersed interface method: numerical solutions of PDEs involving interfaces and irregular domains*, SIAM, Philadelphia, PA, 2006.

[24] W. MCLEAN, *Strongly Elliptic Systems and Boundary Integral Equations*, Cambridge University Press, Cambridge, UK, 2000.

[25] P. MONK, *Finite Element Methods for Maxwell's Equations*, Clarendon Press, Oxford, 2003.

[26] J. NÉDÉLEC, *Mixed finite elements in* $\mathbb{R}^3$, Numer. Math., 35 (1980), pp. 315–341.

[27] P.-O. PERSSON AND G. STRANG, *A simple mesh generator in MATLAB*, SIAM Review, 46 (2004), pp. 329–345.

[28] M. PLUM AND C. WIENERS, *Optimal a priori estimates for interface problems*, Numer. Math., 95 (2003), pp. 735–759.

Research Reports

No.	Authors/Title
09-04	*R. Hiptmair, J. Li, J. Zou* Convergence analysis of Finite Element Methods for H(curl;Ω)-elliptic interface problems
09-03	*A. Chernov, T. von Petersdorff, C. Schwab* Exponential convergence of *hp* quadrature for integral operators with Gevrey kernels
09-02	*A. Cohen, R. DeVore, C. Schwab* Convergence rates of best N-term Galerkin approximations for a class of elliptic sPDEs
09-01	*B. Adhikari, R. Alam, D. Kressner* Structured eigenvalue condition numbers and linearizations for matrix polynomials
08-32	*R. Sperb* Optimal bounds in reaction diffusion problems with variable diffusion coefficient
08-31	*R. Hiptmair* Discrete compactness for p-version of tetrahedral edge elements
08-30	*H. Heumann, R. Hiptmair* Extrusion contraction upwind schemes for convection-diffusion problems
08-29	*N. Hilber, C. Schwab, C. Winter* Variational sensitivity analysis of parametric Markovian market models
08-28	*K. Schmidt, S. Tordeux* Asymptotic modelling of conductive thin sheets
08-27	*R. Hiptmair, P.R. Kotiuga, S. Tordeux* Self-adjoint curl operator
08-26	*N. Reich* Wavelet compression of anisotropic integrodifferential operators on sparse tensor product spaces
08-25	*N. Reich* Anisotropic operator symbols arising from multivariate jump processes
08-24	*N. Reich* Wavelet compression of integral operators on sparse tensor spaces; Construction, consistency and asymptotically optimal complexity
08-23	*F. Liu, N. Reich, A. Zhou* Two-scale Finite Element discretizations for infinitesimal generators of jump processes in finance